Material Matters™

VOLUME 18 • NUMBER 2

Special Issue: Biomedical Research in China

Rational Design of ECMs Toward Cancer Immunotherapy

Approaches to the Design of Lipid-based Nanocarriers for mRNA Delivery

Recent Advances in 3D-Bioprinting-based Drug Screening: A Mini Review and Perspective

Material Matters™
VOL. 18, NO. 2 • 2023

Introduction

Elizabeth Aisenbrey, Ph.D.
Global Product Manager
– Biomedical Materials

Welcome to the 2023 special issue of Material Matters™ focusing on cutting-edge biomaterials research in China. In this issue, we explore advancements in drug delivery, 3D bioprinting, and translational biomaterials that address key challenges in healthcare, biomedical sciences, and engineering.

In our first article, **Professor Shaohua Ma** (Tsinghua Shenzhen International Graduate School) explores engineering extracellular matrix (ECM) biomaterials to improve cancer immunotherapy. ECMs, complex tissue structures comprised of proteins, polysaccharides, and other biomolecules, present biophysical and biochemical cues that can directly impact and drive cell behavior. Using synthetic or natural polymers, ECMs can be strategically designed to interact appropriately with immune or cancer cells and elicit optimal immunomodulatory behavior to improve existing cancer therapies. This review article delves into suitable ECM biomaterials, their interactions with immune cells, and their applications in cancer immunotherapy.

Our second article by **Professor Xiangrong Song** (Sichuan University) investigates design approaches to lipid-based nanocarriers for mRNA delivery. Lipid nanoparticles (LNPs) are the most prominent mRNA delivery system due to their high efficiency, low toxicity, and FDA approval. Despite their success in the clinic, further research and development into the design and engineering of lipids and LNPs is needed to improve delivery and efficiency. This review article helps guide future LNP research and development by exploring key areas of improvement, including lipid structure, surface modification and functionalization, prescription optimization, and administration route.

In our final article, **Professor Xiuli Zhang** (Soochow University) offers a glimpse into the current state of 3D bioprinting for drug screening applications. Though currently in its infancy, 3D bioprinting provides a unique advantage in drug screening because it combines biomaterials and living cells to create a three-dimensional in vitro tissue-like model that better mimics the physiological complexity of human native tissues than 2D cell culture and eliminates animal testing. This review article highlights recent progress in 3D bioprinted tissue models, summarizes the advancements of 3D bioprinting in drug discovery, and discusses the further of 3D bioprinting compared to other techniques such as organoids and organ-on-a-chip models.

Each article in this special issue of Material Matters™ concludes with a curated list of related products available from MilliporeSigma. For more information and additional product offerings, please visit us at SigmaAldrich.com/matsci. If you have any new product suggestions, questions, comments, or new ideas for future Material Matters, please contact us at *SigmaAldrich.com/technicalservice.*

About the Cover

In recent years, China has become a leader in cutting-edge biomedical research as the need to develop biomaterials that can be taken from the bench to the clinic grows. This special issue of Material Matters showcases recent advances in biomaterials research in China. As the cover depicts, this issue includes mini-reviews and perspectives on the diverse field of biomaterials research, highlighting the latest research findings in hot topic areas such as 3D bioprinting and drug delivery. Collectively, this special issue provides a glimpse into China's innovations in biomaterials and their instrumental role in propelling the field forward.

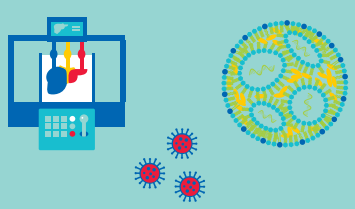

EMD Millipore Corporation
400 Summit Drive
Burlington, MA 01803
Phone (978) 762-5100

To Place Orders / Customer Service
Contact your local office or visit
SigmaAldrich.com/order

Technical Service
Contact your local office or visit
SigmaAldrich.com/techinfo

General Correspondence
Contact your local office or visit
SigmaAldrich.com/techinfo

Subscriptions
Request your FREE subscription to *Material Matters™* at **SigmaAldrich.com/mm**

The entire *Material Matters™* archive is available at **SigmaAldrich.com/mm**

Material Matters™ (ISSN 1933-9631) is a publication of Merck KGaA, Darmstadt, Germany and/or its affiliates

Table of Contents

Articles

Featured Products

Your Material Matters

Bryce P. Nelson, Ph.D.
Head of Chemical Synthesis, Discovery Chemistry & Materials Science
Science & Lab Solutions

Dr. Liwei Hui, Dr. Ipshita Menon, and Dr. Maryam Zaroudi, R&D Formulation Scientists at MilliporeSigma, a business of Merck KGaA, Darmstadt, Germany, are developing novel polymeric and lipid-based drug delivery formulations to add to the NanoFabTx™ Drug Delivery catalog.

Targeted drug and gene delivery is vital for precision medicine. Currently, there are two commonly used targeting strategies: passive targeting and active targeting. Passive targeting relies on nanoparticle characteristics such as size, shape, and surface chemistry. In contrast, active targeting relies on introducing targeting moieties such as antibodies, peptides, or ligands to the nanoparticle surface to specifically recognize desired receptors, cells, or tissues.

To address targeting, we have introduced our NanoFabTx™ Lipid Mixes for targeted delivery including the NanoFabTx™ - Maleimide Lipid Mix (**933570**), NanoFabTx™ - Azide Lipid Mix (**933620**), NanoFabTx™ - Biotin Lipid Mix (**932612**), and the NanoFabTx™ - Natural and Synthetic Folate Lipid Mixes (**933546** and **933562**).

These lipid mixes can be used to conjugate to targeting moieties such as proteins or antibodies or to target cells that overexpress targeted receptors such as tumor cells.

In addition to formulations, the formulation methods can also influence the targetability of nanoparticles by changing the presentation and concentration of targeting moieties on the surface of nanoparticles. Thereby, we have included multiple step-by-step protocols for lipid nanoparticle or liposome preparation using traditional methods and microfluidics with the NanoFabTx™ microfluidic – nano device kit (**911593**) to allow for highly tunable and reproducible nanoparticle preparation. Stay tuned as we introduce more NanoFabTx™ Lipid Mixes for targeted delivery soon!

Name	Cat. No.
NanoFabTx™ - Maleimide Lipid Mix	**933570**
NanoFabTx™ - Azide Lipid Mix	**933620**
NanoFabTx™ - Biotin Lipid Mix	**932612**
NanoFabTx™ - NTA Lipid Mix	**933554**
NanoFabTx™ - Natural Folate Lipid Mix	**933546**
NanoFabTx™ - Synthetic Folate Lipid Mix	**933562**
NanoFabTx™ microfluidic – nano device kit	**911593**

References:

(1) Menon, I.; Zaroudi, M.; Zhang, Y.; Aisenbrey, E.; Hui, L. *Mater. Today Adv.* **2022**, *16*, 100299. DOI: 10.1016/j.mtadv.2022.100299.
(2) Castro, R.; Aisenbrey, E.; Hui, L. *Nanomed.* **2023**, 18 (7), 589–597. DOI: 10.2217/nnm-2023-0052.

EVERYTHING BUT THE KITCHEN SINK

Comprehensive biodegradable polymers for drug delivery

Biodegradable polymers for drug delivery research. Our materials will help you achieve controlled and targeted delivery of therapeutic agents (e.g. APIs, genetic material, peptides, vaccines, and antibiotics).

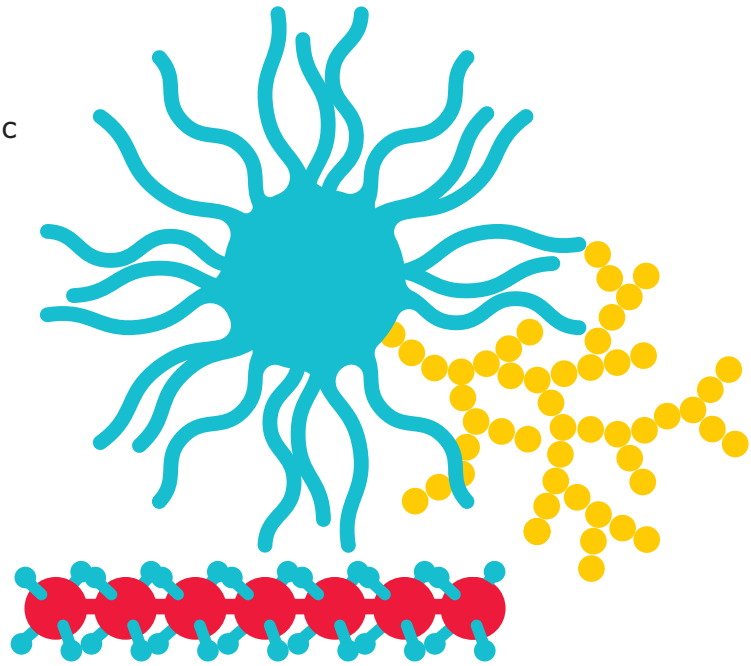

We offer the following classes of high-purity biodegradable polymers for your research needs:

- Poly (lactide-co-glycolide) copolymers (PLGA)
- Poly(lactic acid) (PLA)
- Poly(caprolactone) (PCL)
- Amphiphilic block copolymers
- End-functionalized biodegradable polymers

For more information, please visit:
SigmaAldrich.com/BioPoly

Sigma-Aldrich®
Lab & Production Materials

Rational Design of ECMs Toward Cancer Immunotherapy

Yu Zhang and Shaohua Ma*

Institute of Biopharmaceutical and Health Engineering, Tsinghua Shenzhen International Graduate School, Shenzhen, China
*Email: ma.shaohua@sz.tsinghua.edu.cn

Introduction

Immunotherapy strategies are incredibly critical on the road to clinical cancer treatment. Cancer immunotherapy refers to a treatment that activates or artificially optimizes the immune system to recognize and attack cancer cells.[1–4] Cancer immunotherapy provides several advantages over conventional treatment methods like surgery,[5] radiotherapy,[6] chemotherapy,[7] and other drugs that directly eliminate tumor cells. These benefits include the ability to precisely target cancer cells, enhance long-term efficacy, minimize side effects in terms of both frequency and severity and have the potential for combination with other therapies. Immunotherapies commonly used by clinics involve the following strategies: cell-based immunotherapies including chimeric antigen receptor (CAR)-modified T cell therapy,[9] CAR NK cell therapy,[10] and other immune cell-based therapies; immune checkpoint blockade[11–13] which is among the most frequently used cancer immunotherapy in clinical trials;[14] and tumor vaccines, including human papillomavirus (HPV) and hepatitis B (HBV) vaccines.[15–17] Other infrequently used immunotherapies include cytokine therapies[18] and bacterial therapies.[19] In some clinical trials, immunotherapy is combined with other treatments such as radioisotope therapy,[20] chemotherapy,[21] photodynamic,[22] and ultrasound therapy[23] to target patient-specific diseases with optimal strategies for maximizing performance.

Furthermore, in recent years, the Food and Drug Administration (FDA) has approved various immune drugs and immune cell therapy strategies for the treatment of diverse types of cancer. For example, the HPV vaccine has been widely inoculated;[24] pembrolizumab has been approved for non-small cell lung cancer (NSCLC),[25] nivolumab and ipilimumab have been approved for renal carcinoma,[26] and CAR-T therapy has been approved for certain types of lymphoma and leukemia.[26] Moreover, the number of FDA-approved cancer immunotherapy treatments is increasing annually.[27–29]

Despite its advantages, many diseases cannot be treated by immunotherapy.[30] For instance, cancer antigens are often not effectively delivered to immune cells, the efficiency of immune cell activation and proliferation is too low, and artificial cells (e.g., CAR-T cells) show over-immunization in clinical trials, which can threaten solid tumor patients' lives. Meanwhile, other concerns such as safety, efficiency, accuracy, and autoimmune reactions remain to be considered.[31] Immunosenescence,[32] known as age-related alterations in the immune system, has long been a subject of discussion regarding their impact on the heightened susceptibility to cancer among the terminal cancer patients and elderly population.[33] They are also unavoidable factors. Therefore, it is important to note that the effectiveness of these strategies may vary depending on the specific type of cancer, the stage of the disease, and individual patient factors. Ongoing research and clinical trials continuously explore and refine these approaches to improve immunotherapy efficiency.

Extracellular matrices (ECM) are complex networks of proteins and polysaccharides that provide structural and biochemical support to cells and tissues. ECMs with good biocompatibility and immunogenicity can induce the maturation and expansion of immune cells and provide a way for immune regulation through their design. Engineering approaches utilizing the ECM can enhance the effectiveness of immune therapy, either directly or indirectly. By manipulating the physical and chemical properties of biomaterials, engineered ECM can serve as frameworks or injectable carriers,

allowing for adjustment of the immune response and improving the effectiveness of tumor immunotherapy within the body.[34] In this context, we will focus on the relationships between ECMs, immune reactions, and cancer therapy, as well as the role of ECMs in enhancing cancer immunotherapy. This will encompass an examination of the material types, the strategic design of materials for controlling cancer immunotherapy through biophysical and biochemical cues, as well as the prevalent or emerging applications of biomaterials in the field.

Immunomodulatory ECMs

To further explore cancer immunotherapy, it is essential to develop appropriate ECMs that enable optimal interaction with immune cells. This involves employing fundamental strategies to enhance the immune response by adjusting the infiltration, activity, and quantity of immune cells.

Synthetic ECMs

Synthetic ECMs can be divided into biodegradable and nonbiodegradable types. We will put first attention on the common-used synthetic ECMs such as poly(lactic-co-glycolic acid) (PLGA),[35] polyvinyl alcohol (PVA),[35] polyethyleneimine (PEI),[36] and poly(beta-amino-ester) (PBAE).[36] Some artificial polymers show excellent biocompatibility, low cytotoxicity, and robust mechanical properties. Consequently, these polymers find extensive applications in the encapsulation and delivery systems of (immune) drugs and vaccines.

Poly (lactic-co-glycolic acid) (PLGA) is a degradable synthetic material consisting of lactic acid and glycolic acid monomers. The production of non-toxic lactic acid and glycolic acid upon degradation indicates favorable biocompatibility. PLGA can provide a stable encapsulation matrix due to its excellent mechanical properties that can preserve the structural integrity and activity of the antibody/virus/bacteria. Therefore, PLGA is routinely employed as a vaccine carrier for injection. It also shows excellent interactions with immune cells. It is reported that PLGA stimulates dendritic cells (DCs) to express several CD molecules, including CD40, CD80, and CD83, which can mature and activate T cells.[37] Due to its good performance, PLGA is approved by FDA for clinical trials.[38]

Polyvinyl alcohol (PVA) is a soluble synthetic polymer made from the polymerization of vinyl alcohol monomers. PVA shows excellent stability and low toxicity, commonly used as a stabilizer. It plays a crucial role in drug delivery for tumor treatment by enhancing drug stability, improving bioavailability, controlling release rates, and enhancing the biocompatibility of the delivery systems. The concentration of PVA and the combination of factors, including particle precursors, degree of drug loading, and solvent type, can determine stability.[39]

Additionally, poly(caprolactone) (PCL), poly(methyl methacrylate) (PMMA), and poly(ε-caprolactone-co-lactide) (PCLA) can also be used for stabilizing and delivering immune drugs, virus or RNA.[40]

Polyethylenimine (PEI) is a synthetic polymer made from the polymerization of ethylene imide monomers. Its high molecular weight and favorable solid electric properties make it highly immunogenic and can form stable complexes with nucleic acid.[41] It can activate immune cells and deliver many RNA vaccines after implanting.[42] It was reported that PEI has the ability to activate macrophages and enhance the production of IL-12, promoting the cell response of type 1 T helper.[43] Also, research shows that combining it with cationic dextran induces a highly effective antitumor effect by reverting myeloid-derived suppressor cells (MDSCs) from immunosuppressive to immunostimulatory, illustrating the significant advantages of cationic properties.[44]

Hydrophobic poly(beta-amino-ester) (PBAE) was first known as a widely used drug delivery cationic polymer with good degradability. Then, it is reported that its immunomodulation ability, including DC activation, stimulation of immune cell expansion, and antigen presentation, will depend on its formulation.[45] Single-free polymers do not show any activation on immune cells, while the assembled particles using PBAE exhibit strong DC activation.

Besides, similar cationic polymers, including poly-L-lysine (PLL), poly(amidoamine) (PAMAM), and Polyvinylpyrrolidone (PVP), have similar principles with PEI and PBAE.

Natural ECMs

Cancer immunotherapy development frequently involves the utilization of biopolymers derived from natural or renewable sources, such as chitosan, alginate, collagen, dextran, and hyaluronic acid. Compared with synthetic ECMs, natural ECMs can be readily adapted for conjugation with various therapeutic agents and targeting ligands based on the desired therapeutic objective.[46] Unlike the high stiffness of other scaffold materials, alginate, collagen, and hyaluronic acid[47] are primarily used as injectable biomaterials due to their highly deformable properties.[48]

Chitosan is a polysaccharide extracted from the shell of crustaceans such as shrimp, crabs, and shellfish. It has been widely used in cancer immunotherapy and *in-situ* vaccine delivery because of its high immunogenicity derived from its fundamental properties, including positive charge, relatively low biodegradability, and easily recognizable polysaccharide structures by toll-like receptors (TLRs) on immune cells. Scaffolds made from chitosan can drive immune responses of cells within or around the scaffold due to its attractive adjuvant properties and ability to trigger host innate immunity.[49] Additionally, chitosan can be modified with biochemical molecules to achieve long-term activation. For example, loading the antigens in chitosan microneedles can induce a high antibody level for 18 weeks with superior antigen immunogenicity because of the continued antigen release and chitosan's adjuvanticity.[50] Chitosan may soon become the most promising ECM for immune therapy because of its unique immunogenicity among natural polymers.

Alginate, a marine-derived natural polymer, has linear structures consisting of β-D-mannuronic acid (M) and α-L-guluronic acid (G),

arranged in consecutive M or G blocks or alternating MG blocks.[51] Alginate is available in multiple forms with varying quality, viscosity (low, medium, or high), and molecular weight (low or high).[52] It is hydrophilic, water-soluble, thickens under neutral conditions, and forms a hydrogel when exposed to polyvalent cations.[53] Its anionic nature, dependent on pH, allows it to interact with cationic polyelectrolytes, making it convenient for cell loading.[53] Alone or in combination with other natural or synthetic polymers, alginate has been recognized as an efficient polymer for loading therapeutic cargo for antitumor treatment.[54] Despite variations in endotoxin content depending on purity, alginate is generally stable and biocompatible, making it a safe ECM for immune drug and vaccine delivery.[55]

Collagen is a triple helix protein with muscular rigidity found in all living organisms. Collagen has excellent biocompatibility and can encapsulate drugs or biomolecules, allowing them to bind to receptors on cancer cells. If the collagen-encapsulated drugs are taken up by the cancer cells, the drug particles will be released. Additionally, collagen scaffolds contain a specific binding domain for type I collagen, enabling the release of fusion proteins. Immunoconjugate-directed targeting of cancer collagen can be effectively used for targeted anticancer therapy.[56] Furthermore, collagen is deeply involved in immune processes. Macrophages activated by chemical signals such as IL-10 and TGF-β express collagen VI, leading to a harder ECM and different immune responses.[57] Therefore, proper use of collagen may be one of the critical points to immune regulation.

Dextran, a neutral complex composed of glucan, with α-1, six glycosidic bonds between glucose monomers, along with branches formed by α-1, 4, α-1, 3, and α-1, 2 linkages,[58] has various advantages for the production of biomaterials with good biodegradability, biocompatibility, and excellent solubility.[59] *In vivo* studies on the biocompatibility of dextran biomaterials have been conducted and demonstrate that they do not induce a toxic response in the human body.[60] Dextran-based materials can also undergo enzymatic and chemical degradation in the small intestine and stomach, which makes them an effective oral drug delivery system for encapsulated molecules.[61] The three secondary hydroxyl groups make it appropriate for chemical modification, and the chemically modified dextran derivatives exhibit diverse properties.[62,63] What's more, through conjugation, dextran has the ability to activate immune cells and enhance the immunogenicity of antigens, particularly tumor antigens.[64,65] Therefore, dextran is a promising ECM in cancer immunotherapy.

Hyaluronic acid (HA) is a naturally occurring linear polysaccharide consisting of N-acetyl-D-glucosamine and D-glucuronic acid units.[66] The most frequently used chemical modifications of hyaluronic acid are the functionalization of the carboxyl and hydroxyl groups, which can generally be used to extend the retention time of hyaluronic acid-based therapeutic agents.[67] *In vivo* experiments show hyaluronic acid-based implants have suitable biocompatibility and can ensure good anticancer effectiveness.[68] HA has unique properties, such as its 3D porous network structure, favorable biodegradability and biocompatibility, and biogenic hydrogel material properties. On this account, HA has been popularly used in antitumor drug delivery by utilizing the affinity of hyaluronic acid for binding with overexpressed CD44 molecules on the surface of tumor cells.[69] Moreover, HA can be widely applied in cancer vaccines to enhance clinical translation by promoting antigen uptake and presentation by antigen-presenting cells (APCs) such as dendritic cells (DCs), as well as improving the efficiency of $CD8^+$ T cell killing.[70]

Inorganic materials. Some inorganic materials, including silica, carbon, and metal, can be immunoregulators in clinical prevention and treatment.[71] Like chitosan, many cations like Mn^{2+} can also activate the innate immune response, inducing IRF3 phosphorylation and type I-IFN production.[72] Combining Mn^{2+} with anti-PD-1 antibodies can essentially reduce the required antibody dose due to the enhancement of antitumor efficiency.[73]

Interactions Between ECM and Immune Cells

Immunogenicity is the prime consideration for designing the supramolecular biomaterials utilized *in vivo*. However, the rules for maximizing or alleviating immunogenicity in immunotherapies require further investigation.[74] Biochemical and biophysical cues from the tissue microenvironment play a crucial role in guiding immune responses and influencing the behaviors of immune cells, such as their initiation and proliferation.[75]

Biophysical Cues

ECMs' physical cues offer crucial tools to tune immune reactions. They strongly correlate with cell morphology, aggregation, migration, activation or proliferation, temporary phenotype changes, and even permanent genetic expression changes.[76] To better investigate the biophysical cues' influence on immune cell behavior, metabolic reprogramming and downstream effects can broaden new opportunities for fostering these relationships.[77]

Mechanical properties. Changes in the mechanical properties, including matrix rigidity, can affect immune cells' behaviors.[78,79] Immune cells can sense and respond to external cues through integrins,[80] ion channels,[81] and cytoskeletal components.[82] For example, when macrophages sense substrate rigidity, they will modulate their behavior, including eliciting phagocytosis,[83,84] ROS production,[85]cell morphology,[86] and inflammatory-related cytokines secretion.[84,87-89] Stiffer ECMs limit inside immune cell migration while promoting immune cell activation processes. For example, macrophages cultured on stiffer fibrin hydrogels show more secretion of tumor necrosis factor (TNF) and interleukin-6 (IL-6) in response to LPS stimulation.[88] It should also be noted that stiffer ECMs can also slow signal transduction, worsen inflammation, and cause additional damage.

Besides ECM regulation, immune cells can also affect ECM stiffness. Some researchers reported that immune cells could express transforming growth factor-B (TGF-β), promoting fibroblast

aggregation and producing stiffer ECM. On the other hand, macrophages can also uptake or degrade collagen by secreting enzymes.[57]

In summary, substrate stiffness plays a role in immune cell behavior, such as T cell spread,[90] proliferation,[91] and cytokine secretion,[92] and immune cells play a role in substrate stiffness by tuning ECMs via expressing factors or proteins.[57] Moreover, all of these processes are dynamic, so a clear understanding of the interactions between ECM stiffness and the immune system activity cycle will be vital in investigating better immunotherapies in the future.

Electrical properties. Immune cells, especially T cells, are sensitive to positively charged surfaces. Since cell membranes are negatively charged, suspended T cells can aggregate rapidly on the cationic ECM surface. Besides, cationic hydrophilic ECMs, which can form cellular internalization by electrostatic interaction, usually have a higher adjuvanticity and benefit DCs or myeloid cells' stimulated maturation. The antigen-presenting process happens after cells interact with the cationic polymer backbone and negative proteoglycans.[93] Wen et al. have provided a valuable strategy for designing potential immunogenicity. They illustrate that a positive surface charge enhances the uptake of fibrillated peptides by antigen-presenting cells (APCs), which initiates the immune response.[94] After that, the cargo presented by scaffold biomaterial is presented on the APC's primary histocompatibility complex class II molecules, thus enhancing both T cell and antibody responses. Additionally, Hao et al. have developed a new chitosan-based vaccine delivery strategy. They utilized a negatively charged virus loaded in chitosan and Calcium-ion-containing ECM that is positively charged to recruit sufficient immune cells, including T and B cells, and activate the immune system. They properly utilized ECM properties to aggregate and activate sufficient immune cells successfully.[95] Further, quaternary chitosan, an improved variant of chitosan that exhibits enhanced solubility in water compared to traditional chitosan due to the introduction of positive charges in its molecular structure, demonstrates more substantial immunoregulatory properties, as the positive charges enable effective interaction with the negative charges.

Other external stimuli. In specific cases, immune cell behavior can be pre-designed by focusing on modulating material surface properties. Chen et al. conclude that surface topography affects macrophage behavior, providing insights into how topographical features can modulate the foreign body response and cellular interactions, such as cell adhesion *in vivo*, without needing bioactive substances.[96] Additionally, ultrasound can offer external energy to improve immunotherapy. Clinical trials have found that ultrasound therapy combined with immunotherapy results in better treatment outcomes.[97] In part, this may be due to external physical interruptions inducing the random release of encapsulated cargo.[98–100]

Consequently, physical cues show strong capabilities for changing physiological processes, and we can control these cells' behavior easily by tuning these physical properties. However, other unclear biophysical cues remain to be further explored, as shown in **Figure 1.**

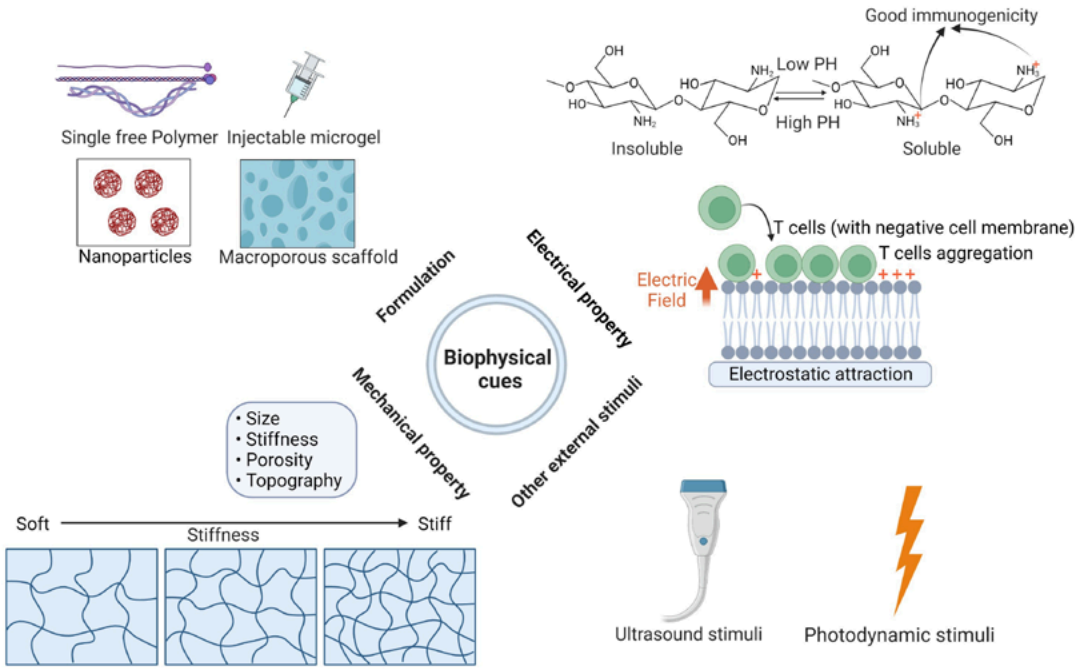

Figure 1. Biophysical cues on interactions between ECM and immune cells. Biophysical cues in the interactions between the extracellular matrix (ECM) and immune cells encompass various aspects, such as formulation (e.g., single free polymer, injectable microgel, nanoparticles, and macroporous scaffold), electrical properties (including ion charge and electrostatic attraction), as well as other external stimuli (such as ultrasound and photodynamic stimuli), which collectively influence immune cell behavior and responses within the ECM environment

Bio-chemical Cues

Polymer-based design. ECMs' molecular structure and chemical groups may play an immunoregulatory role.[36] For instance, rice hull polysaccharides (RHPS), which show potential for reducing tumor growth through upregulating splenic cytotoxicity and infiltration of NK cells in colon tumors, have been recognized to regulate and activate innate immunity in mice.[101] Similarly, molecular structure plays a role in mRNA vaccine delivery, as seen with the superior ionizable lipid biomaterials.[102] Anderson and co-workers have also proposed that lipids with heterocyclic structures can provoke adequate STING-based CDs maturation and an active immune response, which means higher antitumor efficacy.[103]

As for the molecular weight effect, take hyaluronan as an example. HA can be used to activate DCs for priming allogeneic T cells in the classic TIRAP pathway,[104] but the induction and infiltration of DCs triggered by hyaluronan will vanish when the molecular weight of HA exceeds 800 kDa.[105] When it comes to immunogenic molecular structures, greater molecular weight corresponds to an increased number of antigenic sites and a more intricate structure, ultimately leading to heightened immunogenicity. Factors such as molecular structure and molecular weight can potentially be used to aggregate more immune cells and activate the immune system.

Adjuvant. An adjuvant can be added to tune the immunogenicity of scaffold biomaterials or injectable hydrogels. Chitosan, for instance, has been utilized as an adjuvant for stimulating APCs. A bioinspired HA-base system consisting of positively charged N-trimethyl chitosan (TMC) and negatively charged γ-PGA was used to encapsulate and deliver a model subunit vaccine ovalbumin (OVA). After injection, the loaded hydrogel was devoured by APCs and induced an antigen-specific antibody response.[106] Other adjuvants, such as CpG, an oligonucleotide that also belongs to an immune adjuvant, have been found to enhance tumor antigens after combination therapy when delivered in a sodium alginate-based hydrogel loaded with catalase, CpG, and iodine.[20] Lastly, adjuvants can be added to synthetic hydrogel materials, such as PLG. Due to the excellent biocompatibility of PLG-based material, some adjuvants, including Trehalose 6,6′-dimycolate (TDM), can also be added to increase their immunogenicity for a better immunotherapy effect.[107]

Surface modification. Surface modification can be used to functionalize various biomaterials. The swelling and degradation characteristics of a scaffold play a significant role in governing the release pharmacokinetics of the cargo it carries. These can be designed by changing their oxidation ability and crosslinking parameters such as crosslinker length, degradability, and density.[108] The electrostatic and hydrophobic-hydrophilic interactions between cargo and scaffolds can also be designed to retain biomolecules.[109–112] Poly(γ-glutamic acid) (γ-PGA), for instance, has been known to induce innate and adaptive immune responses, and antigen internalization, DC activation, and other series of immune responses are connected with its hydrophobicity. After grafting PGA with L-phenylalanine ethyl ester to increase the hydrophobicity, the production of TNF-α, IL-6, and IL-12 is vastly increased, resulting in a more robust DC activation.[113]

One of the emerging strategies to enhance the efficacy of cancer immunotherapy is to engineer ECMs that can modulate the immune microenvironment. ECMs can also be modified with specific ligands and antibodies to activate immune cells and improve immunotherapy efficiency.[114] ECMs decorated with anti-CD3 and anti-CD28 antibodies can stimulate T cells and induce their proliferation and cytotoxicity.[115–117] This approach can potentially overcome the immunosuppressive effects of the tumor microenvironment and enhance the antitumor response. Therefore, chemically modified ECM-based immunotherapy is a promising platform for cancer treatment that can leverage the natural interactions between cells and their microenvironment. Moreover, ECMs can also be combined with other immunomodulatory agents, such as cytokines, checkpoint inhibitors, or cancer vaccines, to boost the immune system.[118–120]

Matrix-binding/loading molecular conjugates. Matrix-binding molecules are molecules that can bind to the matrix surrounding cancer cells, thereby precisely delivering drugs to the location of the cancer cells. Ishihara et al. have engineered a conjugate[13] that can improve antitumor immunity, reduce ICI side effects, and decrease tumor growth speed in murine breast cancer.[118] Though advantageous, conjugates have not been proven to eradicate tumors in all murine models. The exploration of a localized method for immune checkpoint blockade involves the conjugation of checkpoint blockade antibodies with a highly potent peptide derived from placenta growth factor-2 (PlGF-2123-144). This conjugation resulted in enhanced tissue retention and reduced systemic side effects. In murine melanoma and breast cancer tumor models, peritumoral injections of PlGF-2123-144-conjugated antibodies delayed tumor growth, prolonged survival, and increased infiltration of activated T cells in tumors.[119] This approach of using engineered ECM-binding antibodies presents a promising and safer strategy for checkpoint blockade. Although it is superior in delivering the drug into the tumor ECM accurately, with higher stability and retention, research investigating matrix-binding conjugates is still in the early preclinical stages. Future clinical trials are needed to ensure efficacy and safety.

In summary, tuning biochemical factors is the most immediate and effective method for adjusting immune cells/systems' behavior. Different ECM components, adjuvants, and surface chemical groups can lead to different pathways or factors (e.g., CD-X, interleukin-X, TNF, etc.) that activate or inhibit immune cells. **(Figure 2)**

Applications of Materials in Cancer Immunotherapy

In the cancer immunotherapy workflow, biomaterials can be used *in vitro* for immune cell culture, expansion, activation, and *in vivo* for drug delivery and immune cell activation. To better activate or increase the aggregation of immune cells within the tumor and decrease the off-target effects, researchers have proposed several

novel strategies for enhancing the delivery process, including implantable scaffolds, injectable/spreadable hydrogels, transdermal microneedles, nanoparticles and matrix-binding molecular conjugates.[120]. Researchers also utilize engineered approaches to activate or screen immune cells *in vivo*. Herein, *in vivo* and *in vitro* applications will be discussed, respectively **(Figure 3)**.

In vivo Studies

Localized immunotherapy delivery can perform its role by regulating anticancer immune response and helping reduce drug doses.[121–123] On one hand, novel strategies for designing ECMs aim to reduce off-target immunotoxicity while maintaining the drug accumulation speed, retention, and control release. On the other

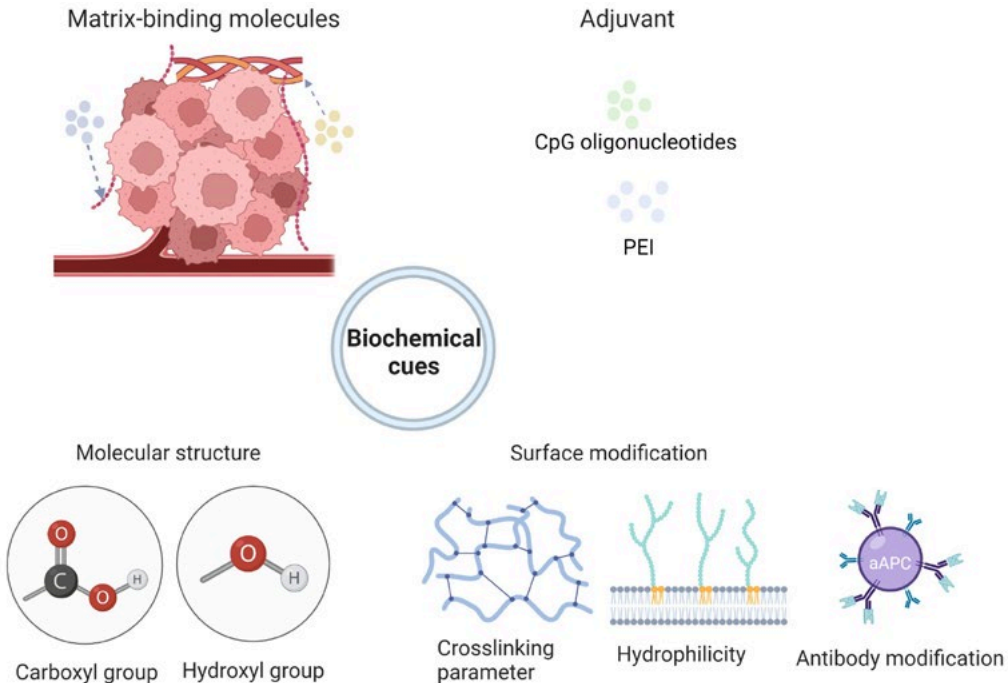

Figure 2. Interactions and biochemical cues between ECM and immune cells. The interactions and biochemical cues between the extracellular matrix (ECM) and immune cells involve various factors, including matrix-binding molecules, adjuvants, molecular structures (such as carboxyl and hydroxyl groups), and surface modifications (such as crosslinking parameters, hydrophilicity, and antibody modifications), all of which play a crucial role in influencing immune cell behavior and responses within the ECM microenvironment.

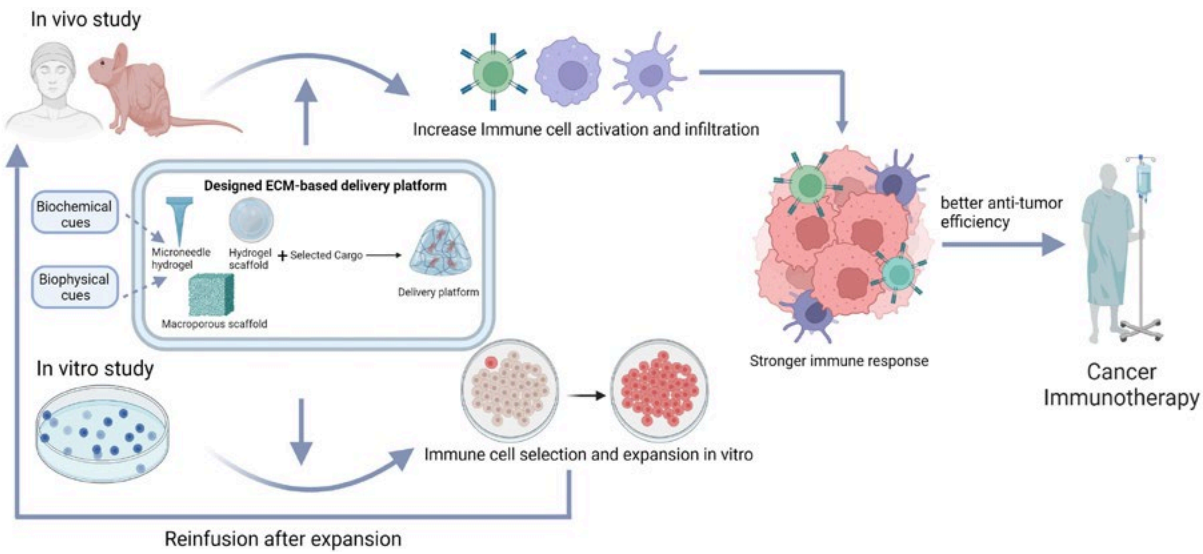

Figure 3. Engineered ECM-based delivery platform used in *in vivo* and *in vitro* studies for enhanced treatment. The utilization of engineered ECM-based delivery platforms combining selected cargo with scaffolds or microgels offers a promising approach for enhancing treatment outcomes, enabling improved immune cell selection and expansion *in vitro* and subsequent reinfusion into the in *vivo body*, leading to enhanced immune cell activation, infiltration, and ultimately improved anti-tumor efficacy in cancer immunotherapy.

hand, implantable ECMs can also be designed with relatively high immunogenicity to aggregate autologous immune cells and activate the immune system *in vivo*. ECMs designed for localized delivery of immunotherapy can be divided into the following categories: implantable biomaterials scaffolds, injectable hydrogel-based material, transdermal microneedles, and matrix-binding molecular conjugates.[124–127]

Implantable Scaffold

The implantable scaffold is a macroscale porous biomaterial loaded with chemical components and biological cells implanted into a host.[128] The most commonly used polymeric biomaterials for scaffolds include poly(lactide-co-glycolide) (PLG),[129] alginates,[130] polyglycolide and porcine gelatin,[131] collagen, and hyaluronic acid (HA).[132] The role of an implantable scaffold is to release the encapsulated cargo to the targeted tissue area in a controlled fashion. Then, the ECM-based implant uses its physical and chemical properties or autologous immunogenicity to recruit immune cells, enhancing immune responses and tumor suppression.[48]

There are numerous examples of utilizing implantable scaffolds to influence the immune response and enhance immunotherapy. For instance, PLG scaffolds have been used to carry and release Granulocyte-macrophage colony-stimulating factor (GMCSF) to attract, aggregate, and induce the maturation of DCs after implantation.[133,134] The post-mature DCs then migrate to draining lymph nodes to present antigens, ultimately resulting in T cell expansion and a higher immune response.[135] Hao et al. designed a chitosan-alginate-based implantable scaffold to recruit immune cells via the material's immunogenicity and positive charge. Upon recruiting cells, the vaccine within the scaffold was administered, subsequently activating these cells and resulting in successful vaccine delivery.[95] Further, Tyrel et al. demonstrated that co-delivery of IFN gene (STING) agonists with CAR T cells within an alginate scaffold not only eradicates tumors with higher efficiency compared to direct delivery but also eliminates tumor cells that are not recognized by the lymphocytes in adoptive cell transfer immunotherapy.[139]

Injectable/spreadable Hydrogel-based Biomaterial

Injectable/spreadable hydrogels are soft, absorbent, 3D structures that maintain biodegradability, injectability, and controllable physiochemical properties. Hydrogels have a high potential for immobilizing biological factors due to their hydrated environment. It has also been found to reduce side effects and vastly improve the antitumor immune response when used in therapeutic delivery.[140] They have also been found to be suitable for combination therapy with chemotherapy or radioisotope therapy.[141]

Hydrogel delivery of RNA is specifically of interest because it offers fewer off-target effects, localized and sustained delivery, and the ability to maintain RNA bioactivity.[142] Many studies have demonstrated the validity of RNA vaccines in immunologically

Table 1: Different implantable ECMs for cancer immunotherapy.

Encapsulation	Cargo	Tumor model / Target disease	Therapeutic strategy
PLG	GM-CSF	Murine and human colorectal tumors	DC-based cancer Vaccine[153]
PLG	GM-CSF+ VpG-ODN+ tumor-associated antigen	Murine melanoma model	DC-based cancer vaccine[154]
HA-PCLA	GM-CSF+ immunomodulatory factor (pOVA)	Human lung carcinoma	Cell-based immunotherapy[155]
Alginate	CAR-T cell + stimulator of IFN genes (STING) agonists	Murine Pancreatic tumors	CAR T therapy[156]
Graphene oxide +polyethylenimine	mRNA+ Adjuvants R848	B16-OVA melanoma model	mRNA vaccine, Protect mRNA from degradation in cancer immunotherapy[144]
Polyamidoamine (PAMAM) +dextran aldehyde	SiRNA+ oligopeptide-terminated poly (β-aminoester) (pBAE) nanoparticles	Human breast cancer	Drug delivery of bioactive agents to combat cancer[157]
Fibrin	Calcium carbonate nanoparticles loaded with the anti-CD47 antibody	B16F10 murine melanoma	Inhibit tumor recurrence after surgery[158]
Fibrin	CTX+anti-PD-L1	Murine models of TNBC 4T1 breast cancer and ID8 ovarian cancer	Inhibit tumor recurrence after surgery[159]
PVA+TSPBA	Chemotherapeutic gemcitabine and anti-PD-L1	B16F10 melanoma and 4T1 breast tumor models	Combination therapy for reducing ROS in TME[160]
Oligochitosan+ nano Calcium carbonate	Zika virus (ZIKV)	Acute respiratory syndrome coronavirus 2	Live virus Vaccine therapy[161]

insensitive cancers, including glioblastoma and pancreatic ductal adenocarcinoma (PDAC).[143] To solve the problem of the low efficiency for released RNA vaccine entering the APCs, Yin and colleagues reported that an in situ transformable hydrogel, which is formed by graphene oxide and polyethylenimine, can vastly increase the number of $CD8^+$ T cells and inhibit the tumor growth by preventing mRNA degradation after administration.[144]

Transdermal Microneedle

Due to the possibility of hepatic first-pass extraction, transdermal microneedles (MN) are outstanding alternatives to implanted devices when treating skin cancers such as melanoma. Darge et al. have reported an interpenetrating polymer network hydrogel containing lipopolysaccharide (LPS) and doxorubicin (DOX) for synergistic cancer immunotherapy. *In vivo* experiments on glioma-bearing mice confirmed enhanced immune response and tumor inhibition with dual drug-loaded microneedles (MNs) (LPS/DOX@MNs), showing synergistic immunochemotherapeutic effects. MN-mediated combined immunochemotherapy offers localized and sustained drug delivery, a promising strategy for efficient synergistic therapy.[152]

Note: GM-CSF: a recruitment factor that recruits and stimulates specific dendritic cell populations;[135] CpG-ODNs: CpG oligodeoxynucleotides, one kind of adjuvants which derived directly from bacteria;[162] HA-PCLA: poly(ε-caprolactone-co-lactide) ester-functionalized hyaluronic acid; CTX: cyclophosphamide, a small molecule drug; Anti-PD-L1: immune-checkpoint-blocking monoclonal antibody; PVA: polyvinyl alcohol; TSPBA: a ROS-labile linker.

Implanted ECMs offer promising fresh ideas in the field of immunotherapy; however, some challenges still exist, including weak mechanical properties. ECM transplantation may lead to excessive immune activation (immune hyperactivation), resulting in inflammation or autoimmune disorders. This can potentially damage host tissues and limit the application of ECM transplantation. Also, ECM transplantation can disrupt the balance and regulation of the immune system. The components and characteristics of ECM may affect the activation, proliferation, differentiation, and function of immune cells, thereby interfering with normal immune responses. Further long-term studies are needed to assess the lasting impact of ECM transplantation on the immune system and its safety. Particularly in human applications, more clinical research is required to determine the optimal sources of ECM, processing methods, and transplantation strategies. Despite the potential challenges, excellent biocompatibility, biodegradability, and controllability via the design elements listed above, biomaterials will continue to play a role in biomedical applications, especially in cancer immunotherapy.

In vitro Studies

Immunotherapy requires many ECMs-related preparation steps, such as encapsulation for protecting vaccines and immune drug loading. Above all, ECMs can often offer engineered solutions to real medical problems that pure biological technologies, such as autologous immune cell expansion and hyper immunity in immunotherapy, cannot.

Immune Cell Activation and Expansion

With the development of CAR-T, CAR-NK, and similar technologies, immune cell autologous transplantation is increasingly essential.[156,157] However, primary immune cells, especially T cells, have limited activation and expansion efficiency, restricting their applications in immune cell therapy.

ECM-based microcarriers are tiny beads that can be effectively used to culture cells in three-dimensional suspension, including T cells. They provide a large surface area for T cell aggregation and growth and can be modified with various biomolecules to influence cell behavior. Coating specific antigens, such as anti-CD3, anti-CD19, and anti-CD28, onto microcarriers can serve as a method of creating artificial antigen-presenting cells (APCs). These APCs play a crucial role in stimulating the expansion and activation of T cells.[157] Microcarriers dramatically increase the proliferation rate of primary cells and allow immune cell therapy through autologous transplantation. This approach can overcome some of the limitations of conventional methods, such as low efficiency, high cost, and safety issues.

Furthermore, researchers have documented that antibodies targeting immune checkpoint molecules such as CTLA-4 or PD-1 can augment the priming or activity of endogenous T cell responses against tumor antigens.[158] Certain antigens possess the ability to selectively activate T cells, promoting the elimination of tumor cells.[159] Consequently, the combination of ECM-based carriers with these antigens holds promise as a viable approach to expanding T cells on a significant scale. It is important to note that excessive activation can result in T-cell exhaustion. Therefore, the development of an ECM with favorable immunogenicity is crucial to facilitate the expansion of immune cells for cancer immune cell therapy.

Immunoadsorption

Immunoadsorption is a treatment method operated *in vitro* that usually needs to be repeated to continuously regulate immune molecules in the body. Fixed antibodies or other biomolecules on ECMs can bind and remove wastes from blood or other fluid extensively and effectively. Matrix-based immunoadsorption has many clinical applications, especially in treating immune-related diseases.[160–162] For example, immunoadsorption can be used to remove excess or abnormal autoantibodies in the body, such as systemic lupus erythematosus and myasthenia gravis.[160] By removing active immune molecules, immunoadsorption can help regulate the function of the immune system for such applications as the prevention of transplant rejection and immunodeficiency diseases.[163,164] Additionally, it can apply to allergy treatment[165] and immune blood diseases.[166] ECM-based immunotherapy techniques offer novel solutions for engineered clinical applications and are poised to continually advance application processes in this field.

However, limitations, such as the safety and bioavailability of ECM-based drug administration still exist,[167] and more exploration on the interaction mechanism between ECMs and immune cells in clinical immunotherapies remains to be done to enhance their efficiency.

Conclusion and Outlook

ECMs have been demonstrated to play a crucial role in promoting the clinical application of cancer immunotherapy. Immunomodulatory ECMs can be used *in vitro* and *in vivo* to build a superiorly designed ECM-based delivery platform, promote and control immune cell behavior through ECM interactions, and ultimately improve cancer treatments.

Firstly, from the perspective and direction of immunomodulatory ECM design strategies for improving tumor treatment efficiency, ECMs and some composites with strong inherent immunogenicity can directly stimulate the immune system. Secondly, interactions between ECMs and immune cells can be a significant breakthrough for material design. Immunogenicity can be enhanced by altering surface properties such as ECM stiffness and the types of molecular functional groups, as well as the charged capabilities of polymer main chain or side chain groups. Such stimulation triggers the activation of immune cells, bolstering immune responses and enhancing the efficacy of tumor immunotherapy. Natural ECMs with high biocompatibility and degradability, and typically low immunogenicity, can be modified by incorporating adjuvants to enhance immunogenicity while preserving biocompatibility.

Additionally, ECM adjustments, including electrostatic properties, can modulate the interactions between ECM formation and degradation, cargo loading and release, and immune cell behaviors. The adjustment of ECMs can enhance the efficiency of targeted drug or vaccine delivery to specific tumor sites and improve drug release efficiency, thus enhancing the effectiveness of tumor immunotherapy. Moreover, the framework components, or injectable ECMs, can also influence the efficiency of immune responses. By implementing individualized and patient-specific ECM-based therapeutic approaches based on tumor characteristics and patient status, the toxicities associated with these therapies can be effectively reduced, and therapy efficiency can be improved. Finally, determining how to implement the designed ECM-based delivery platform into the *in vivo* and *in vitro* studies will be critical to understanding a better clinical treatment outcome.

On the one hand, by utilizing their immune regulatory effect, ECMs can first serve as carriers for gene molecules and targeted drugs. They can be designed as artificial antigen-presenting cells to directly activate specific immune cell pathways, thereby enhancing immune cell activation and improving antitumor proliferation efficiency. These biomaterials can also be used as a framework or injectable materials for transplantation, aiming to enhance immune cell infiltration, activation, and proliferation, thus boosting the immune response, and improving tumor therapeutic outcomes. Alternatively, immune cell expansion can be carried out through *in vitro* studies, allowing for their subsequent reinfusion into the body. This approach aims to elicit a stronger immune response and enhance the effectiveness of cancer treatment.

Based on the current research status, the field of cancer immunotherapy shows immense potential but requires further optimization. There are several potential application directions for future development. Firstly, one crucial direction is manufacturing immune cells based on genetic engineering, where immune cells are genetically modified to enhance their antitumor activity on a large scale and in a short time. It requires a suitable ECM design to properly activate immune cells that can also prevent immune cell exhaustion. Secondly, using matrix materials in combined immunotherapy presents additional possibilities, including customized and engineered approaches. By utilizing specific ECMs, such as biopolymers or synthetic materials, combined with immunotherapy and immune systems, multi-methods of combination therapy, such as chemotherapy, photothermal therapy, and cell therapy, can be realized, and the effectiveness of immune-based treatments can be improved. Another potential direction is developing tumor-immune tissue engineering using optimized composite materials. Current ECMs often provide only a single function, necessitating the exploration of new matrix materials or the development of new composite materials to offer more comprehensive functionalities. This approach may mimic and reconstruct the interactions between tumors and immune cells using suitable composite materials to enhance immune therapeutic effects. Additionally, ECM-based technologies show a promising future in cell quality control that can be applied to cancer immune cell therapy.

According to the properties previously mentioned, several other points must be considered when designing ECMs to control immune cell function. At the very beginning, after defining destination applications and cargo agents **(Figure 4)**, the design of ECMs used for injectable hydrogel should consider biocompatibility, complexity, and accessibility for clinical translation and gelation kinetics during hydrogel-loaded cargo administration. Considering the ECM's properties when forming injectable materials such as hydrogel, the biomaterials require the correct mechanical properties to pass through a needle to allow the liquid or gel to be implanted into the designated area.[168] The physicochemical properties play a crucial role in the physiological activities of immune cells, including cytokine expression, phenotype, and maturation, although the underlying mechanisms are not fully understood. Notably, other interaction mechanisms between the ECM, immune cells, and tumors remain unclear and may lead to application issues. Natural polymer-synthetic polymer hybrid composites have been introduced to overcome individual ECMs' drawbacks by synergizing their advantages and compensating for their limitations. For instance, Chitosan/γ-PGA composites can form a new material with stronger antigenicity. This hybrid material reportedly gains the ability to revert immunosuppressive macrophages to their stimulatory phenotype, activate the immature DCs in tumors, and promote the proliferation and infiltration of $CD4^+$ and $CD8^+$ cells, ultimately inducing an apparent higher immune response than chitosan

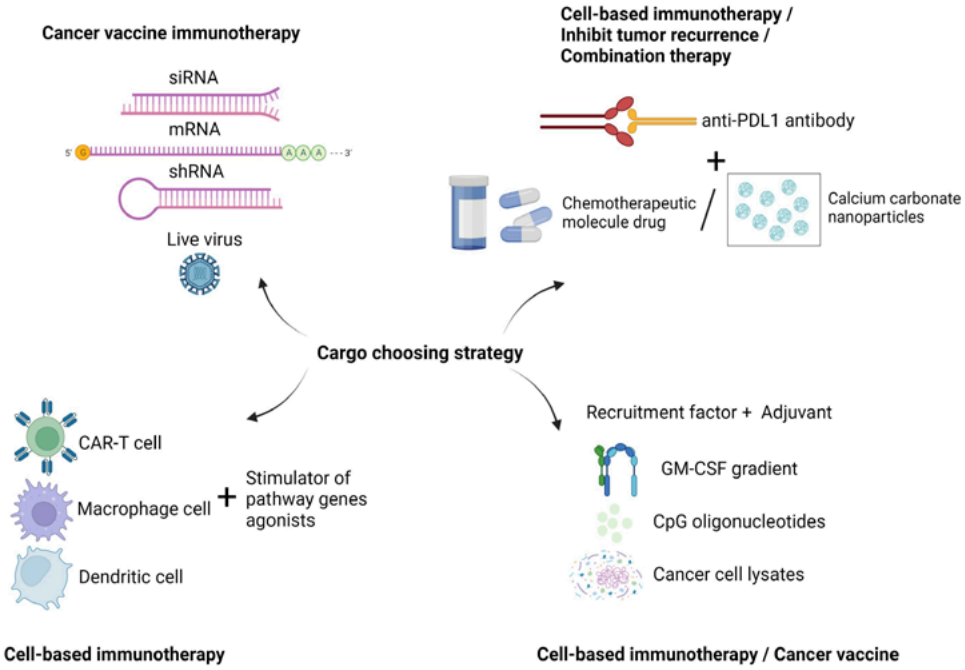

Figure 4. Cargo choosing strategies based on target cancer models and therapeutic methods. The selection of cargo for cancer immunotherapies, such as siRNA, mRNA, and shRNA, depends on the target cancer model and therapeutic methods, while combinations of antibodies, chemotherapeutic molecules, and cell-based immunotherapy offer potential approaches for inhibiting tumor recurrence, combination therapy, and enhancing immune response through immune cell stimulation and recruitment factors.

or γ-PGA alone.[169,170] For PEG hydrogels, the interwoven porous structure has mechanical stability and can be used for transporting cytokines/chemokines, but its biocompatibility and interactions with cells are much lower than those of natural polymers. That said, when combined with a collagen matrix, they can act as a scaffold for loading the migrated T and dendritic cells. The composite opens up more possibilities with much stronger capabilities than those of the original materials and can act as a novel engineering platform for cancer immunotherapy.[171]

As for the *in vitro* applications, it may be concluded that ECM-based immunoadsorption can be used to bind and remove waste, such as hypersensitive immune cells, viruses, and bacteria. This may be beneficial for existing immune cell therapy applications. For instance, patients with solid tumors treated with CAR-T cells can develop severe pneumonia caused by CAR-T cells' hyper immunity or cytokine overexpression (cytokine release syndrome).[172] ECM-based immunoadsorption, an engineered method to screen and remove the hypersensitive or unqualified CAR-T cells, may reduce the damage caused by excessive aggression of CAR-T cells and offer a combined therapy solution. Moreover, ECM properties can be fine-tuned and adjusted to improve binding and removing efficiency. If a proper ECM-immunoadsorption system can be built, a more accurate and mature CAR-T method will accelerate research in solid tumor therapies.

Finally, integrating diverse technologies is crucial in pursuing these developmental pathways. These technologies must involve the optimization of material properties, such as physicochemical characteristics, stability, and biocompatibility. This refinement ensures that the materials can be controlled effectively and safely in practical applications. Additionally, incorporating algorithms and controlled release techniques enables precise drug delivery and release, thereby enhancing the efficacy of treatments. ECMs offer engineered solutions that expand the range of application scenarios and possibilities for advancing the clinical implementation of cancer immunotherapy. Moreover, the mechanism of interaction between ECMs and immune cells, which remains incompletely understood, highlights the need for future research and underscores the significant potential for practical applications.

Reference

(1) Palucka, A. K.; Coussens, L. M. *Cell* **2016**, *164* (6), 1233–1247. DOI:10.1016/j.cell.2016.01.049

(2) Papaioannou, N. E.; Beniata, O. V.; Vitsos, P.; Tsitsilonis, O.; Samara, P. *Ann Transl. Med.* **2016**, *4* (14). DOI:10.21037/atm.2016.04.01

(3) Ribas, A. *N. Engl. J. Med.* **2015**, *373* (16), 1490–1492. DOI:10.1056/NEJMp1510079

(4) Klevorn, L. E.; Teague, R. M. *Trends Immunol* **2016**, *37* (6), 354–363. DOI:10.1016/j.it.2016.03.010

(5) Park, C. G.; Hartl, C. A.; Schmid, D.; Carmona, E. M.; Kim, H. J.; Goldberg, M. S. *Sci. Transl. Med.* **2018**, *10* (433). DOI:10.1126/scitranslmed.aar1916

(6) Ngwa, W.; Irabor, O. C.; Schoenfeld, J. D.; Hesser, J.; Demaria, S.; Formenti, S. C. *Nat. Rev. Cancer* **2018**, *18* (5), 313–322. DOI:10.1038/nrc.2018.6

(7) DeVita Jr., V. T.; Chu, E. *J Cancer Res.* **2008**, *68* (21), 8643–8653. DOI:10.1158/0008-5472.CAN-07-6611

(8) Fukumura, D.; Kloepper, J.; Amoozgar, Z.; Duda, D. G.; Jain, R. K. *Nat. Rev. Clin. Oncol.* **2018**, *15* (5), 325–340. DOI:10.1038/nrclinonc.2018.29

(9) Curran, K. J.; Brentjens, R. J. *J. Clin. Oncol.* **2015**, *33* (15), 1703–1706. DOI:10.1200/JCO.2014.60.3449

(10) Gong, H.; Ham,J. D.; Hu, G.; Xie, G.; Vergara, J.; Liang, Y.; Ali, A.; Tarannum, M.; Donner, H.; Baginska, J.; Abdulhamid, Y.; Dinh, K.; Soiffer, R. J.; Ritz, J.; Glimcher, L. H.; Romee, R. *Proc. Natl. Acad. Sci. U.S.A* **2020**, *59*, 102975. DOI: 10.1073/pnas.2122379119

(11) Ribas, A.; Wolchok, J. D. *Science* **2018**, *359* (6382), 1350–1355. DOI:10.1126/science.aar4060

(12) Moynihan, K. D.; et al. *Nat. Med.* **2016**, *22* (12), 1402–1420. DOI:10.1038/nm.4200
(13) Ishihara, J.; Fukunaga, K.; Ishihara, A.; Larsson, H. M.; Potin, L.; Hosseinchi, P.; Galliverti, G.; Swartz, M. A.; Hubbell, J. A., *Sci. Transl. Med.* **2017**, *9* (415). DOI:10.1126/scitranslmed.aan0401
(14) Weber, J. *Semin. Oncol.* **2010**, *37*, 430–439. DOI: 10.1053/j.seminoncol.2010.09.005
(15) Fesnak, A. D.; June, C. H.; Levine, B. L. *Nat. Rev. Cancer* **2016**, *16* (9), 566–581. DOI:10.1038/nrc.2016.97
(16) Ali, O. A.; Verbeke, C.; Johnson, C.; Sands, R. W.; Lewin, S. A.; White, D.; Doherty, E.; Dranoff, G.; Mooney, D. J. *Cancer Res.* **2014**, *74* (6), 1670–1681. DOI:10.1158/0008-5472.CAN-13-0777
(17) Goldberg, M. S. *Cell* **2015**, *161* (2), 201–204. DOI:10.1016/j.cell.2015.03.037
(18) Berraondo, P.; Sanmamed, M. F.; Ochoa, M. C.; Etxeberria, I.; Aznar, M. A.; Pérez-Gracia, J. L.; Rodríguez-Ruiz, M. E.; Ponz-Sarvise, M.; Castañón, E.; Melero, I. *Br. J. Cancer* **2019**, *120* (1), 6–15. DOI:10.1038/s41416-018-0328-y
(19) Huang, X.; Pan, J.; Xu, F.; Shao, B.; Wang, Y.; Guo, X.; Zhou, S. *Advanced Science* **2021**, *8* (7), 2003572. DOI:10.1002/advs.202003572
(20) Chao, Y; Xu, L; Liang, C; Feng, L; Xu, J; Dong, Z; Tian, L.; Yi, X.; Yang, K.; Liu, Z. *Nat. Biomed. Eng.* **2018**, *2*, 611-621. DOI:10.1038/s41551-018-0262-6
(21) Yu, W.-D.; Sun, G.; Li, J.; Xu, J.; Wang, X. *Cancer Lett.* **2019**, ***452***, 66–70. DOI:10.1016/j.canlet.2019.02.048
(22) Ji, B.; Wei, M.; Yang, B. *Theranostics* **2022**, *12* (1), 434. DOI:10.7150/thno.67300
(23) Unga, J.; Hashida, M. *Adv. Drug Deliv. Rev.* **2014**, *72*, 144–153. DOI:10.1016/j.addr.2014.03.004
(24) Wong, N. C. H. *Commun. Rep.* **2016,** *29* (3), 127–138. DOI:10.1080/08934215.2015.1083599
(25) Pai-Scherf, L., et al. *Oncologist* **2017**, *22* (11), 1392–1399. DOI:10.1634/theoncologist.2017-0078
(26) Vaddepally, R. K.; Kharel, P.; Pandey, R.; Garje, R.; Chandra, A. B., *Cancers (Basel)* **2020**, *12* (3), 738. DOI:10.3390/cancers12030738
(27) Haslam, A.; Prasad, V. *JAMA Netw Open.* **2019**, *2* (5), e192535. DOI:10.1001/jamanetworkopen.2019.2535
(28) Hargadon, K. M.; Johnson, C. E.; Williams, C. J. *Int Immunopharmacol.* **2018**, *62*, 29–39. DOI:10.1016/j.intimp.2018.06.001
(29) Twomey, J. D.; Zhang, B. *AAPS J* **2021**, *23* (2), 39. DOI:10.1208/s12248-021-00574-0
(30) Yang, Y. *J. Clin. Invest.* **2015**, *125* (9), 3335–3337. DOI:10.1172/JCI83871
(31) Taefehshokr, N.; Baradaran, B.; Baghbanzadeh, A.; Taefehshokr, S. *Immunobiology* **2020**, *225* (2), 151875. DOI:10.1016/j.imbio.2019.11.010
(32) Tarazona, R., et al. *Cancer Immunol.* **2017**, *66* (2), 233–245. DOI:10.1007/s00262-016-1882-x
(33) Tan, S.; Li, D.; Zhu, X. *Biomed. Pharmacother.* **2020**, *124*, 109821. DOI:10.1016/j.biopha.2020.109821
(34) Yang, F.; Shi, K.; Jia, Y.-P.; Hao, Y.; Peng, J.-R.; Qian, Z.-Y. *Acta Pharmacol. Sin.* **2020**, *41* (7), 911–927. DOI:10.1038/s41401-020-0372-z
(35) Gardner, A. B.; Lee, S. K.; Woods, E. C.; Acharya, A. P. *Biomed. Res. Int.* **2013**, *2013*, 732182. DOI:10.1155/2013/732182
(36) Chen, W.; Li, C.; Jiang, X. *Small Methods* **2023**, *7* (5), 2201404. DOI:10.1002/smtd.202201404
(37) Park, J.; Gerber, M. H.; Babensee, J. E. *J. Biomed. Mater. Res. A* **2015**, *103* (1), 170–184. DOI:10.1002/jbm.a.35150
(38) Gentile, P.; Chiono, V.; Carmagnola, I.; Hatton, P. V. *Int. J. Mol. Sci.* **2014**, *15* (3), 3640–3659. DOI:10.3390/ijms15033640
(39) Li, W.; Liu, Z.; Fontana, F.; Ding, Y.; Liu, D.; Hirvonen, J. T.; Santos, H. A. *J. Adv. Mater.* **2018**, *30* (24), 1703740. DOI:10.1002/adma.201703740
(40) Soni, V.; Pandey, V.; Asati, S.; Gour, V.; Tekade, R. K. Biodegradable block copolymers and their applications for drug delivery. *In Basic Fundamentals of Drug Delivery*, Elsevier: **2019**; pp 401–447. DOI:10.1016/B978-0-12-817909-3.00011-X
(41) Pandey, Abhijeet P.; Sawant, Krutika K., *Materials Science and Engineering: C* **2016, *68***, 904–918. DOI:10.1016/j.msec.2016.07.066
(42) Aigner, A.; Fischer, D.; Merdan, T.; Brus, C.; Kissel, T.; Czubayko, F. *Gene Ther.* **2002**, *9* (24), 1700–1707. DOI:10.1038/sj.gt.3301839
(43) Li, J.; Jiang, X.; Li, H.; Gelinsky, M.; Gu, Z. *Adv. Mater.* **2021**, *33* (12), e2004172. DOI:10.1002/adma.202004172
(44) He, W.; Liang, P.; Guo, G.; Huang, Z.; Niu, Y.; Dong, L.; Wang, C.; Zhang, J. *Sci. Rep.* **2016**, *6*, 24506. DOI:10.1038/srep24506
(45) Andorko, J. I.; Jewell, C. M. *Bioeng. Transl. Med.* **2017**, *2* (2), 139–155. DOI:10.1002/btm2.10063
(46) Wong, K. H.; Lu, A.; Chen, X.; Yang, Z. *Molecules* **2020**, *25* (16), 3620. DOI:10.3390/molecules25163620
(47) Hixon, K. R.; Lu, T.; Sell, S. A. *Acta Biomater.* **2017**, *62*, 29–41. DOI:10.1016/j.actbio.2017.08.033
(48) Koshy, S. T.; Ferrante, T. C.; Lewin, S. A.; Mooney, D. J. *Biomater.* **2014**, *35* (8), 2477–2487. DOI:10.1016/j.biomaterials.2013.11.044
(49) Gong, N, et al. *Nat. Nanotechnol.* **2020**, *15* (12), 1053–1064. DOI:10.1038/s41565-020-00782-3
(50) Singh, B.; Maharjan, S.; Sindurakar, P.; Cho, K. H.; Choi, Y. J.; Cho, C. S. *Int. J. Mol. Sci.* **2018**, *19* (11), 3639. DOI:10.3390/ijms19113639
(51) Tomić, S. L.; Babić Radić, M. M.; Vuković, J. S.; Filipović, V. V.; Nikodinovic-Runic, J.; Vukomanović, M. *Mar. Drugs* **2023**, *21* (3), 177. DOI:10.3390/md21030177
(52) Heiligenstein, S.; Cucchiarini, M.; Laschke, M. W.; Bohle, R. M.; Kohn, D.; Menger, M. D.; Madry, H. *Tissue Engi. Part C, Methods* **2011**, *17* (8), 829–842. DOI:10.1089/ten.tec.2010.0681
(53) Smith, A. M.; Senior, J. J. *Advances in Biochemical Engineering/Biotechnology* **2021**, *178*, 37–61. DOI:10.1007/10_2020_161
(54) Tomić, S. L.; Babić Radić, M. M.; Vuković, J. S.; Filipović, V. V.; Nikodinovic-Runic, J.; Vukomanović, M. *Mar. Drugs* **2023**, *21* (3), 177. DOI:10.3390/md21030177
(55) Lee, K. Y.; Mooney, D. J. *Prog. Polym. Sci.* **2012**, *37* (1), 106–126. DOI:10.1016/j.progpolymsci.2011.06.003
(56) Lee, C. H.; Singla, A.; Lee, Y. *Int. J. Pharm.* **2001**, *221* (1), 1–22. DOI:10.1016/S0378-5173(01)00691-3
(57) Sutherland, T. E.; Dyer, D. P.; Allen, J. E. *Science* **2023**, *379* (6633), eabp8964. DOI: 10.1126/science.abp8964
(58) Heinze, T.; Liebert, T.; Heublein, B.; Hornig, S. *Adv. Polym. Sci.* **2006**, *205*, 199–291. DOI:10.1007/12_100
(59) Anirudhan, T. S.; Binusreejayan *Int. J. Biol. Macromol.* **2016**, *88*, 222–235. DOI:10.1016/j.ijbiomac.2016.03.040
(60) Cadee, J. A.; van Luyn, M. J. A.; Brouwer, L. A.; Plantinga, J. A.; van Wachem, P. B.; de Groot, C. J.; den Otter, W.; Hennink, W. E. *J. Biomed. Mater. Res.* **2000**, *50* (3), 397–404. DOI:10.1002/(SICI)1097-4636(20000605)50:3<397::AID-JBM14>3.0.CO;2-A
(61) Hu, Q. B.; Lu, Y. J.; Luo, Y. C. *Carbohydr. Polym.* **2021**, *264*, 117999. DOI:10.1016/j.carbpol.2021.117999
(62) Maia, João & Evangelista, Marta & Gil, Helena & Ferreira, Lino. (2014). Dextran-based materials for biomedical applications.
(63) Van Tomme, S. R.; Hennink, W. E. *Expert Rev. Med. Devices* **2007**, *4* (2), 147–164. DOI:10.1586/17434440.4.2.147
(64) Wang, H.; Han, X.; Dong, Z.; Xu, J.; Wang, J.; Liu, Z. *Adv. Funct. Mater.* **2019**, *29* (29), 1902440. DOI:10.1002/adfm.201902440
(65) Zhang, W.; An, M.; Xi, J.; Liu, H. *Bioconjugate Chem.* **2017**, *28* (7), 1993–2000. DOI:10.1021/acs.bioconjchem.7b00313
(66) Cai, J.; Fu, J.; Li, R.; Zhang, F.; Ling, G.; Zhang, P. *Carbohydr. Polym.* **2019**, *208*, 356–364. DOI:10.1016/j.carbpol.2018.12.074
(67) Harrer, D.; Sanchez Armengol, E.; Friedl, J. D.; Jalil, A.; Jelkmann, M.; Leichner, C.; Laffleur, F. *Int. J. Pharm.* **2021**, *601*, 120589. DOI:10.1016/j.ijpharm.2021.120589
(68) Xu, K.; Yao, H.; Fan, D.; Zhou, L.; Wei, S. *Carbohydr. Polym.* **2021**, *254*, 117286. DOI:10.1016/j.carbpol.2020.117286
(69) Fang, Y.; Shi, L.; Duan, Z.; Rohani, S. *Int. J. Biol. Macromol.* **2021**, *189*, 554–566. DOI:10.1016/j.ijbiomac.2021.08.140
(70) Li, X.; Shou, Y.; Tay, A. *Adv. NanoBiomed Res.* **2021**, 189, 554–566. DOI:10.1002/anbr.202000073
(71) Yan, S.; Luo, Z.; Li, Z.; Wang, Y.; Tao, J.; Gong, C.; Liu, X. *Angew.* **2020**, *132* (40), 17484–17495. DOI:10.1002/ange.202002780
(72) Wang, C., et al. *Immunity* **2018**, *48* (4), 675–687.e7. DOI:10.1016/j.immuni.2018.03.017
(73) Lv, Mengze, et al. *Cell Res.* **2020**, *30* (11), 966–979. DOI:10.1038/s41422-020-00395-4
(74) Shae, D.; Baljon, J. J.; Wehbe, M.; Becker, K. W.; Sheehy, T. L.; Wilson, J. T. *J. Leukoc. Biol.* **2020**, *108* (4), 1435–1453. DOI:10.1002/JLB.5BT0119-016R
(75) Du, H.; Bartleson, J. M.; Butenko, S.; Alonso, V.; Liu, W. F.; Winer, D. A.; Butte, M. J. *Nat. Rev. Immunol.* **2023**, *23* (3), 174–188. DOI:10.1038/s41577-022-00761-w
(76) Mariani, E.; Lisignoli, G.; Borzì, R. M.; Pulsatelli, L. *Int. J. Mol. Sci.* **2019**, *20* (3), 636. DOI:10.3390/ijms20030636
(77) Ding, Y.; Wang, Y.; Hu, Q. *Explor.* **2022**, *2* (3), 202110106. DOI:10.1002/exp.20210106
(78) Guimaraes, C. F.; Gasperini, L.; Marques, A. P.; Reis, R. L. *Nat. Rev. Mater.* **2020**, *5* (5), 351–370. DOI:10.1038/s41578-019-0169-1
(79) Paul, C. D.; Hung, W. C.; Wirtz, D.; Konstantopoulos, K., Engineered Models of Confined Cell Migration. In ***Annual Review of Biomedical Engineering, Vol 18***, Yarmush, M. L., Ed. 2016; Vol. 18, pp 159–180. DOI:10.1146/annurev-bioeng-071114-040654
(80) Roy, N. H.; MacKay, J. L.; Robertson, T. F.; Hammer, D. A.; Burkhardt, J. K. *Sci. Signal* **2018**, *11* (560). DOI:10.1126/scisignal.aat3178
(81) Köhler, R.; Heyken, W.-T.; Heinau, P.; Schubert, R.; Si, H.; Kacik, M.; Busch, C.; Grgic, I.; Maier, T.; Hoyer, J. *Arterioscler. Thromb. Vasc. Biol.* **2006**, *26* (7), 1495–1502. DOI:10.1161/01.ATV.0000225698.36212.6a
(82) Huse, Morgan *Nat. Rev. Immunol.* **2017**, *17* (11), 679–690. DOI:0.1038/nri.2017.74
(83) Sridharan, R.; Cavanagh, B.; Cameron, A. R.; Kelly, D. J.; O'Brien, F. J. *Acta Biomater.* **2019**, *89*, 47–59. DOI:10.1016/j.actbio.2019.02.048
(84) Dutta, B.; Goswami, R.; Rahaman, S. O. *Front. Immunol.* **2020**, *11*. DOI:10.3389/fimmu.2020.570195
(85) Geng, J., et al. *Nat. Commun.* **2021**, *12* (1). DOI:10.1038/s41467-021-23683-y

(86) Chen, M.; Zhang, Y.; Zhou, P.; Liu, X.; Zhao, H.; Zhou, X.; Gu, Q.; Li, B.; Zhu, X.; Shi, Q. *Bioact. Mater.* **2020**, *5* (4), 880–890. DOI:10.1016/j.bioactmat.2020.05.004

(87) Atcha, H., et al. *Nat. Commun.* **2021**, *12* (1). DOI:10.1038/s41467-021-23482-5

(88) Meli, Vijaykumar S, et al. *Sci. Adv.* **2020**, *6* (49), eabb8471. DOI:10.1126/sciadv.abb8471

(89) Scheraga, R. G.; Southern, B. D.; Grove, L. M.; Olman, M. A. *Front. Immunol.* **2020**, *11*. DOI:10.3389/fimmu.2020.01211

(90) Wahl, A.; Dinet, C.; Dillard, P.; Nassereddine, A.; Puech, P. H.; Limozin, L.; Sengupta, K. *Proc. Natl. Acad. Sci. U. S. A.* **2019**, *116* (13), 5908–5913. DOI:10.1073/pnas.1811516116

(91) Hickey, J. W., et al. *Adv. Mater.* **2019**, *31* (23), 1807359. DOI:10.1002/adma.201807359

(92) Liu, Y. Y., et al. *Cancer Res.* **2021**, *81* (2), 476–488. DOI:10.1158/0008-5472.CAN-20-2569

(93) Hu, Y.; Gong, X.; Zhang, J.; Chen, F.; Fu, C.; Li, P.; Zou, L.; Zhao, G. *Polymers* **2016**, *8* (4), 99. DOI:10.3390/polym8040099

(94) Wen, Y.; Waltman, A.; Han, H. F.; Collier, J. H. *ACS Nano* **2016**, *10* (10), 9274–9286. DOI:10.1021/acsnano.6b03409

(95) Hao, Haibin, et al. *Nat. Biomed. Eng.* **2023**, *7*, 928–942. DOI:10.1038/s41551-023-01014-4

(96) Chen, S. L.; Jones, J. A.; Xu, Y. G.; Low, H. Y.; Anderson, J. M.; Leong, K. W. *Biomater.* **2010**, *31* (13), 3479–3491. DOI:10.1016/j.biomaterials.2010.01.074

(97) Huebsch, N.; Kearney, C. J.; Zhao, X. H.; Kim, J.; Cezar, C. A.; Suo, Z. G.; Mooney, D. J. *Proc. Natl. Acad. Sci. U.S.A* **2014**, *111* (27), 9762–9767. DOI:10.1073/pnas.1405469111

(98) Hastings, C. L.; Kelly, H. M.; Murphy, M. J.; Barry, F. P.; O'Brien, F. J.; Duffy, G. P. *J. Control. Release* **2012**, *161* (1), 73–80. DOI:10.1016/j.jconrel.2012.04.033

(99) Garbern, J. C.; Minami, E.; Stayton, P. S.; Murry, C. E. *Biomater.* **2011**, *32* (9), 2407–2416. DOI:10.1016/j.biomaterials.2010.11.075

(100) Zhao, X. H.; Kim, J.; Cezar, C. A.; Huebsch, N.; Lee, K.; Bouhadir, K.; Mooney, D. J. *Proc. Natl. Acad. Sci. U.S.A* **2011**, *108* (1), 67–72. DOI:10.1073/pnas.1007862108

(101) Yang, L.-C.; Hsieh, C.-C.; Lin, W.-C. *Carbohydr. Polym.* **2015**, *124*, 150–156. DOI:10.1016/j.carbpol.2015.02.025

(102) Akinc, A., et al. *Nat. Biotechnol.* **2008**, *26* (5), 561–569. DOI:10.1038/nbt1402

(103) Miao, L., et al. *Nat. Biotechnol.* **2019**, *37* (10), 1174–1185. DOI:10.1038/s41587-019-0247-3

(104) Tesar, B. M.; Jiang, D.; Liang, J.; Palmer, S. M.; Noble, P. W.; Goldstein, D. R. *Am. J. Transplant* **2006**, *6* (11), 2622–2635. DOI:10.1111/j.1600-6143.2006.01537.x

(105) Park, J.; Babensee, J. E. *Acta Biomater.* **2012**, *8* (10), 3606–3617. DOI:10.1016/j.actbio.2012.06.006

(106) Korupalli, C.; Pan, W. Y.; Yeh, C. Y.; Chen, P. M.; Mi, F. L.; Tsai, H. W.; Chang, Y.; Wei, H. J.; Sung, H. W. *Biomater.* **2019**, *216*, 119268. DOI:10.1016/j.biomaterials.2019.119268

(107) Khademi, F.; Derakhshan, M.; Yousefi-Avarvand, A.; Tafaghodi, M. *Iran J. Basic Med. Sci.* **2018**, *21* (2), 116–123. DOI:10.22038/IJBMS.2017.22059.5648

(108) Rosales, A. M.; Anseth, K. S. *Nat. Rev. Mater.* **2016**, *1* (2). DOI:10.1038/natrevmats.2015.12

(109) Pakulska, M. M.; Donaghue, I. E.; Obermeyer, J. M.; Tuladhar, A.; McLaughlin, C. K.; Shendruk, T. N.; Shoichet, M. S. *Sci. Adv.* **2016**, *2* (5), e1600519. DOI:10.1126/sciadv.1600519

(110) Sakiyama-Elbert, S. E. *Acta Biomater.* **2014**, *10* (4), 1581–1587. DOI:10.1016/j.actbio.2013.08.045

(111) Kearney, C. J.; Mooney, D. J. *Nat. Mater.* **2013**, *12* (11), 1004–1017. DOI:10.1038/NMAT3758

(112) Larraneta, E.; Stewart, S.; Ervine, M.; Al-Kasasbeh, R.; Donnelly, R. F. *J. Funct. Biomater.* **2018**, *9* (1). DOI:10.3390/jfb9010013

(113) Shima, F.; Akagi, T.; Akashi, M. *Biomater. Sci.* **2014**, *2* (10), 1419–1425. DOI:10.1039/C4BM00140K

(114) Rowley, A. T.; Nagalla, R. R.; Wang, S. W.; Liu, W. F. *Adv. Healthc. Mater.* **2019**, *8* (8), e1801578. DOI:10.1002/adhm.201801578

(115) Shimizu, Y.; van Seventer, G. A.; Ennis, E.; Newman, W.; Horgan, K. J.; Shaw, S. *J. Exp. Med.* **1992**, *175* (2), 577–582. DOI:10.1084/jem.175.2.577

(116) Hickey, J. W., et al. *Adv. Mater.* **2019**, *31* (23), e1807359. DOI:10.1002/adma.201807359

(117) Huang, J. Y.; Cheng, Y. J.; Lin, Y. P.; Lin, H. C.; Su, C. C.; Juliano, R.; Yang, B. C. *J. Immunol.* **2010**, *185* (3), 1450–1459. DOI:10.4049/jimmunol.0901352

(118) Riley, R. S.; June, C. H.; Langer, R.; Mitchell, M. J. *Nat. Rev. Drug Discov.* **2019**, *18* (3), 175–196. DOI:10.1038/s41573-018-0006-z

(119) Ishihara, J.; Fukunaga, K.; Ishihara, A.; Larsson, H. M.; Potin, L.; Hosseinchi, P.; Galliverti, G.; Swartz, M. A.; Hubbell, J. A. *Sci. Transl. Med.* **2017**, *9* (415), eaan0401. DOI:10.1126/scitranslmed.aan0401

(120) Zhao, Z. W.; Zheng, L. Y.; Chen, W. Q.; Weng, W.; Song, J. J.; Ji, J. S. *J. Hematol. Oncol.* **2019**, *12* (1). DOI:10.1186/s13045-019-0817-3

(121) Milling, L.; Zhang, Y.; Irvine, D. J. *Adv. Drug Deliv. Rev.* **2017**, *114*, 79–101. DOI:10.1016/j.addr.2017.05.011

(122) Oh, E.; Oh, J. E.; Hong, J.; Chung, Y.; Lee, Y.; Park, K. D.; Kim, S.; Yun, C. O. *J. Control. Release* **2017**, *259*, 115–127. DOI:10.1016/j.jconrel.2017.03.028

(123) Kwong, B.; Gai, S. A.; Elkhader, J.; Wittrup, K. D.; Irvine, D. J. *Cancer Res.* **2013**, *73* (5), 1547–1558. DOI:10.1158/0008-5472.CAN-12-3343

(124) Xu, J. J.; Xu, B. H.; Tao, J.; Yang, Y. X.; Hu, Y.; Huang, Y. Z. *Small* **2017**, *13* (28). DOI:10.1002/smll.201700666

(125) Prausnitz, M. R. *Adv. Drug Deliv. Rev.* **2004**, *56* (5), 581–587. DOI:10.1016/j.addr.2003.10.023

(126) Weber, J. S.; Mule, J. J. *Nat. Biotechnol.* **2015**, *33* (1), 44–45. DOI:10.1038/nbt.3119

(127) Lei, K. W.; Tang, L. *Biomater. Sci.* **2019**, *7* (3), 733–749. DOI:10.1039/c8bm01470a

(128) Lim, S.; Park, J.; Shim, M. K.; Um, W.; Yoon, H. Y.; Ryu, J. H.; Lim, D. K.; Kim, K. *Theranostics* **2019**, *9* (25), 7906–7923. DOI:10.7150/thno.38425

(129) Ali, O. A.; Lewin, S. A.; Dranoff, G.; Mooney, D. J. *Cancer Immunol. Res.* **2016**, *4* (2), 95–100. DOI:10.1158/2326-6066.CIR-14-0126

(130) Stephan, S. B.; Taber, A. M.; Jileaeva, I.; Pegues, E. P.; Sentman, C. L.; Stephan, M. T. *Nat. Biotechnol.* **2015**, *33* (1), 97–101. DOI:10.1038/nbt.3104

(131) Zhan, Q.; Shen, B. Y.; Fang, Y.; Deng, X. X.; Chen, H.; Jin, J. B.; Peng, C. H.; Li, H. W. *Colloids Surf. B* **2017**, *158*, 469–473. DOI:10.1016/j.colsurfb.2017.07.021

(132) Phuengkham, H.; Song, C.; Um, S. H.; Lim, Y. T. *Adv. Mater.* **2018**, *30* (18). DOI:10.1002/adma.201706719

(133) Metcalf, D. *Nat. Rev. Cancer* **2010**, *10* (6), 425–434. DOI:10.1038/nrc2843

(134) Hercus, T. R.; Thomas, D.; Guthridge, M. A.; Ekert, P. G.; King-Scott, J.; Parker, M. W.; Lopez, A. F. *Blood* **2009**, *114* (7), 1289–1298. DOI:10.1182/blood-2008-12-164004

(135) Ali, O. A.; Emerich, D.; Dranoff, G.; Mooney, D. J. *Sci. Transl. Med.* **2009**, *1* (8), 8ra19. DOI:10.1126/scitranslmed.3000359

(136) Vallet-Regi, M.; Colilla, M.; Gonzalez, B. *Chem. Soc. Rev.* **2011**, *40* (2), 596–607. DOI:10.1039/c0cs00025f

(137) Lee, J. E.; Lee, N.; Kim, T.; Kim, J.; Hyeon, T. *Acc. Chem. Res.* **2011**, *44* (10), 893–902. DOI:10.1021/ar2000259

(138) Nguyen, T. L.; Choi, Y.; Kim, J. *Adv. Mater.* **2019**, *31* (34), 1803953. DOI:10.1002/adma.201803953

(139) Smith, T. T., et al. *J. Clin. Investig.* **2017**, *127* (6), 2176–2191. DOI:10.1172/JCI87624

(140) Qin, J.; Sun, M.; Hu, W.; Cheng, J.; Fan, Z.; Du, J. *Polym. Chem.* **2023**, *14* (7), 793–802. DOI:10.1039/d2py01308h

(141) Ungerleider, J. L.; Christman, K. L. *Stem Cells Transl. Med.* **2014**, *3* (9), 1090–1099. DOI:10.5966/sctm.2014-0049

(142) Zhong, R.; Talebian, S.; Mendes, B. B.; Wallace, G.; Langer, R.; Conde, J.; Shi, J. *Nat. Mater.* **2023**, *22*, 818–831. DOI:10.1038/s41563-023-01472-w

(143) Huff, A. L.; Jaffee, E. M.; Zaidi, N. *J. Clin. Invest.* **2022**, *132* (6), e156211. DOI:10.1172/JCI156211

(144) Yin, Y.; Li, X.; Ma, H.; Zhang, J.; Yu, D.; Zhao, R.; Yu, S.; Nie, G.; Wang, H. *Nano Lett.* **2021**, *21* (5), 2224–2231. DOI:10.1021/acs.nanolett.0c05039

(145) Darge, H. F.; Lee, C.-Y.; Lai, J.-Y.; Lin, S.-Z.; Harn, H.-J.; Chen, Y.-S.; Tsai, H.-C. *Chem. Eng. J.* **2022**, *433*, 134062. DOI:10.1016/j.cej.2021.134062

(146) Dranoff, G. *Immunol. Rev.* **2002**, *188*, 147–54. DOI:10.1034/j.1600-065x.2002.18813.x

(147) Urdinguio, Rocio G., et al. *Cancer Res.* **2013**, *73* (1), 395–405. DOI:10.1158/0008-5472.CAN-12-0806

(148) Duong, H. T. T.; Thambi, T.; Yin, Y.; Kim, S. H.; Nguyen, T. L.; Phan, V. H. G.; Kim, J.; Jeong, J. H.; Lee, D. S. *Biomater.* **2020**, *230*, 119599. DOI:10.1016/j.biomaterials.2019.119599

(149) Smith, T. T., et al. *J. Clin. Invest.* **2017**, *127* (6), 2176–2191. DOI:10.1172/jci87624

(150) Segovia, N.; Pont, M.; Oliva, N.; Ramos, V.; Borrós, S.; Artzi, N. *Adv. Healthc. Mater.* **2015**, *4* (2), 271–280. DOI:10.1002/adhm.201400235

(151) Chen, Q., et al. *Nat. Nanotechnol.* **2019**, *14* (1), 89–97. DOI:10.1038/s41565-018-0319-4

(152) Zhang, L.; Zhou, J.; Hu, L.; Han, X.; Zou, X.; Chen, Q.; Chen, Y.; Liu, Z. *Adv. Funct. Mater.* **2020**, *30* (7), 1906922. DOI:10.1002/adfm.201906922

(153) Erfani, A.; Diaz, A. E.; Doyle, P. S. *Mater. Today* **2023**, *65*, 227–243. DOI:10.1016/j.mattod.2023.03.006

(154) Hao, H., et al. *Nat. Biomed. Eng.* **2023**, *7*, 928–942. DOI:10.1038/s41551-023-01014-4

(155) Weiner, G. J.; Liu, H. M.; Wooldridge, J. E.; Dahle, C. E.; Krieg, A. M. *Proc. Natl. Acad. Sci. U.S.A* **1997**, *94* (20), 10833–10837. DOI:10.1073/pnas.94.20.10833

(156) Shah, U. A.; Mailankody, S. *Best Pract. Res. Clin. Haematol.* **2020**, *33* (1), 101141. DOI:10.1016/j.beha.2020.101141

(157) Dwarshuis, N.; Song, H. W.; Patel, A.; Kotanchek, T.; Roy, K. *bioRxiv* **2019**. DOI:10.1101/646760

(158) Sadelain, M.; Rivière, I.; Riddell, S. *Nature* **2017**, *545* (7655), 423–431. DOI:10.1038/nature22395

(159) Arnaud, M.; et al. *Nat. Biotechnol.* **2022**, *40* (5), 656–660. DOI:10.1038/s41587-021-01072-6
(160) Boedecker, S. C.; et al. **2022**, *37* (1), 70–81. DOI:10.1002/jca.21953
(161) Fuchs, K., et al., *Ther. Apher. Dail.* **2022**, *26* (1), 229–241. DOI:10.1111/1744-9987.13663
(162) Lazaridis, K.; Baltatzidou, V.; Tektonidis, N.; Tzartos, S. J. *J. Neuroimmunol.* **2020**, *339*, 577136. DOI:10.1016/j.jneuroim.2019.577136
(163) Chamling, B., Könemann, S., Dörr, M., Felix, S.B. (**2020**). Immunomodulation and Immunoadsorption in Inflammatory Dilated Cardiomyopathy. In: Caforio, A. (eds) Myocarditis. Springer, Cham. DOI:10.1007/978-3-030-35276-9_15
(164) Raina, R.; Wang, J.; Sharma, A.; Chakraborty, R. *Blood Purif.* **2020**, *49* (5), 513–523. DOI:10.1159/000506277
(165) Arasi, S. et al. *World Allergy Organ. J.* **2023**, *16* (2), 100750. DOI:10.1016/j.waojou.2023.100750
(166) Richter, P.; Fischer, H.; Dörfelt, R. *J. Clin. Apher.* **2021**, *36* (4), 668–672. DOI:10.1002/jca.21913
(167) Taefehshokr, S.; Parhizkar, A.; Hayati, S.; Mousapour, M.; Mahmoudpour, A.; Eleid, L.; Rahmanpour, D.; Fattahi, S.; Shabani, K.; Taefehshokr, N. *Pathol. Res. Pract.* **2022**, **229**, 153723. DOI:10.1016/j.prp.2021.153723
(168) Leach, D. G.; Young, S.; Hartgerink, J. D. *Acta Biomater.* **2019**, ***88***, 15–31. DOI:10.1016/j.actbio.2019.02.016
(169) Castro, F., et al. *Biomater.* **2020**, *257*, 120218. DOI:10.1016/j.biomaterials.2020.120218
(170) Castro, F., et al. *Acta Biomater.* **2017**, *63*, 96–109. DOI:10.1016/j.actbio.2017.09.016
(171) Stachowiak, A. N.; Irvine, D. J. *J. Biomed. Mater. Res. A* **2008**, *85* (3), 815–828. DOI:10.1002/jbm.a.31661
(172) Liu, Y., et al. *J. Immunother.* **2018**, *41* (9), 406–410. DOI:10.1097/CJI.0000000000000243

Natural Polymers

Alginate

Name	Description	Molecular Weight	Contains	Cat. No.
Alginate aldehyde	medium viscosity 20% aldehyde content			**923850**
	medium viscosity 35% aldehyde content			**923842**
Alginate methacrylate	high viscosity degree of methacrylation: 20-40%			**912387**
	medium viscosity degree of methacrylation: 10-30%			**913057**
	low viscosity degree of methacrylation: 10-30%	~75 kDa (Alginate)		**911968**
Low endotoxin alginate	medium viscosity		<10 CFU/g Bioburden <100 EU/g Endotoxin	**919373**
Low endotoxin alginate solution	medium viscosity 0.2 µm, sterile-filtered		<10 EU/g Endotoxin <5 CFU/g Bioburden (Fungal) <5 CFU/g Bioburden (Total Aerobic)	**918652**
Methacrylated alginate	medium viscosity		<10 CFU/g Bioburden (Aerobic) <10 CFU/g Bioburden (Fungal) <100 EU/g Endotoxin	**924482**
mPEG functionalized alginate	low endotoxin 5% PEGylation	PEG average M_n 1k		**920819**
Novatach™ LVM GRGDSP	GRGDSP-peptide coupled high M sodium alginate mannuronate acid content ≥50 %		≤100 EU/g Endotoxins	**4270701**
Novatach™ MVG GRGDSP	GRGDSP-peptide coupled high G high MW sodium alginate guluronic acid contentguluronic acid content ≥60 %		≤100 EU/g Endotoxins	**4270501**
Novatach™ VLVG GRGDSP	GRGDSP-peptide coupled high G low MW sodium alginate guluronic acid contentguluronic acid content ≥60 %		≤100 EU/g Endotoxins	**4270101**
Pronova® SLG 100	sodium alginate solution guluronate monomer units ≥60 %	M_w 150-250 kDa	≤100 EU/g Endotoxins	**4202101**
Pronova® SLG 20	sodium alginate solution guluronate monomer units ≥60 %	M_w 75-150 kDa		**4202001**
Pronova® SLM 100	sodium alginate solution mannuronate monomer units ≥50 %	M_w 150-250 kDa	≤100 EU/g Endotoxins	**4202301**
Pronova® UP LVG	low viscosity sodium alginate guluronate monomer units ≥60 %	M_w 75-200 kDa	≤100 CFU/g Total viable count ≤100 EU/g Endotoxins	**42000001**
Pronova® UP LVM	low viscosity sodium alginate mannuronate monomer units ≥50 %	M_w 75-200 kDa	≤100 CFU/g Total viable count ≤100 EU/g Endotoxins	**42000201**
Pronova® UP MVG	medium viscosity sodium alginate guluronate monomer units ≥60 %	M_w >200 kDa	≤100 CFU/g Total viable count ≤100 EU/g Endotoxins	**42000101**
Pronova® UP MVM	medium viscosity sodium alginate mannuronate monomer units ≥50 %	M_w >200 kDa	≤100 CFU/g Total viable count ≤100 EU/g Endotoxins	**42000301**
Pronova® UP VLVG	very low viscosity sodium alginate guluronate monomer units ≥60 %	M_w <75 kDa	≤100 CFU/g Total viable count ≤100 EU/g Endotoxins	**42000501**
Pronova® UP VLVM	very low viscosity sodium alginate mannuronate monomer units ≥50 %	M_w <75 kDa	≤100 CFU/g Total viable count ≤100 EU/g Endotoxins	**42000601**

Chitosan

Name	Description	Appearance	Cat. No.
Chitosan	from shrimp shells, practical grade	solid	**417963**
	high molecular weight	(Coarse ground flakes and powder)	**419419**
	medium molecular weight	powder	**448877**
	low molecular weight	powder	**448869**
Chitosan glycidyl methacrylate	Degree of methacrylation ~20%		**926167**
Glycol chitosan Methacrylate	Degree of methacrylation ≥45%	white to light yellow/ light brown powder	**926175**
Trimethyl chitosan	high molecular weight degree of quaternization >70%	light yellow to light brown powder	**912034**
	medium molecular weight degree of quaternization: 40-60%	light yellow to light brown powder	**912123**
	low molecular weight degree of quaternization >50%	light yellow to light brown powder	**912700**

Collagen

Name	Description	Cat. No.
Bovine Collagen Solution	Type I, 3 mg/mL, >=95%, sterile filtered, BSE-Free, suitable for biomedical research	**804592**
	Type I, 6 mg/mL, >=95%, sterile filtered, BSE-Free, suitable for biomedical research	**804622**
	Type I, Acid soluble telocollagen, 6 mg/mL, sterile filtered, BSE-Free, suitable for biomedical research	**804614**

Fucoidan

Name	Description	Viscosity	Cat. No.
ProtaSea® Fucoidan	brown seaweed extract	5-10 mPa.s	**G3295-4**

Hyaluronic Acid

Name	Description	Molecular Weight (M_w)	Contains	Cat. No.
Hyaluronic acid adipic dihydrazide (HA-ADH)	white to off-white solid			**930024**
Hyaluronic acid	low viscosity low endotoxin		<10 CFU/g Bioburden <100 EU/g Endotoxin	**924474**
Hyaluronic acid methacrylate	degree of substitution 20-50%	40,000-70,000		**914568**
	degree of substitution 20-50%	140,000-190,000		**914304**
	degree of substitution 20-50%	170,000-250,000		**914800**
	low viscosity low endotoxin		<=10 CFU/g Bioburden (Fungal) <=10 CFU/g Bioburden (Total Aerobic) 100 EU/g Endotoxin	**924490**

Synthetic Polymers

PEG-PLGA

Name	Molecular Weight	Feed Ratio (lactide:glycolide)	Cat. No.
Allyl poly(ethylene glycol)-block-poly (lactide-co-glycolide)	PEG average M_n 5,000 PLGA average M_n 15,000	50:50	**901459**
Amine poly(ethylene glycol)-block-poly (lactide-co-glycolide)	PEG average M_n 5,000 PLGA average M_n 15,000	50:50	**901456**
Biotin-poly(ethylene glycol)-b-poly (lactide-co-glycolide)	PEG average M_n 2,000 PLGA average M_n 10,000	50:50	**909882**
Carboxylic acid poly(ethylene glycol)-block-poly (lactide-co-glycolide)	PEG average M_n 5,000 PLGA average M_n 15,000	50:50	**902071**
Carboxylic acid-poly(ethylene glycol)-b-poly (lactide-co-glycolide)	PEG average M_n 5,000 PLGA average M_n 20,000	50:50	**909858**
Folate-poly(ethylene glycol)-b-poly (lactide-co-glycolide)	PEG average M_n 2,000 PLGA average M_n 10,000	50:50	**909769**
N-Hydroxysuccinimide poly(ethylene glycol)-block-poly (lactide-co-glycolide)	PEG average M_n 5,000 PLGA average M_n 15,000	50:50	**902241**
Maleimide poly(ethylene glycol)-block-poly (lactide-co-glycolide)	PEG average M_n 5,000 PLGA average M_n 15,000	50:50	**925462**
Poly(ethylene glycol) methyl ether-block-poly (lactide-co-glycolide)	PEG average M_n 2,000 PLGA average M_n 10,000	50:50	**913138**
	PEG average M_n 2,000 PLGA average M_n 10,000	80:20	**911399**
	PEG average M_n 2,000 PLGA average M_n 11,500	50:50	**764760**
	PEG average M_n 2,000 PLGA average M_n 3,000	50:50	**900921**
	PEG average M_n 5,000 PLGA average M_n 10,000	80:20	**911410**
	PEG average M_n 5,000 PLGA average M_n 5,000	80:20	**911429**
	PEG average M_n 5,000 PLGA average M_n 10,000	50:50	**900951**
	PEG average M_n 5,000 PLGA average M_n 15,000	50:50	**900948**
	PEG average M_n 5,000 PLGA average M_n 15,000	80:20	**900842**
	PEG average M_n 5,000 PLGA average M_n 20,000	50:50	**900949**
	PEG average M_n 5,000 PLGA average M_n 5,000	50:50	**900950**
	PEG average M_n 5,000 PLGA average M_n 5,000	80:20	**900841**
	PEG average M_n 5,000 PLGA average M_n 55,000	50:50	**764752**
	PEG average M_n 5,000 PLGA average M_n 7,000	50:50	**765139**
	PEG M_n 2,000 PLGA M_n 4,500	65:35	**764825**
Poly(ethylene glycol) methyl ether-block-poly (L-lactide-co-glycolide)	PEG average M_n 5,000 PLGA average M_n 25,000	50:50	**799041**
Poly(ethylene glycol)-block-poly (lactide-alt-glycolide)	PEG average M_n 5,000 PLGA average M_n 15,000	50:50	**925659**
Pyridyl disulfide poly(ethylene glycol)-block-poly (lactide-co-glycolide)	PEG average M_n 5,000 PLGA average M_n 15,000	50:50	**901942**
Redox Responsive Poly(ethylene glycol)-block-poly (lactide-alt-glycolide)	PEG average M_n 5,000 PLGA average M_n 15,000	50:50	**926248**
Thiol poly(ethylene glycol)-block-poly (lactide-co-glycolide)	PEG average M_n 5,000 PLGA average M_n 15,000	50:50	**901941**

PEI

Name	Molecular Weight	Description	Cat. No.
Acetylated branched polyethylenimine solution 20% solution		20% acetylation, suitable for biomedical research	**913235**
Branched PEI-g-PEG	PEG M_n 5,000		**900743**
Branched polyethylenimine solution		2mg/mL aqueous solution, suitable for biomedical research	**913375**
Linear polyethylenimine-block-poly (ethylene glycol)	PEG average M_n 750 PEI average M_n 10,000		**927287**
	PEG average M_n 750 PEI average M_n 15,000		**927317**
	PEG average M_n 2,000 PEI average M_n 10,000		**927295**
	PEG average M_n 2,000 PEI average M_n 20,000		**927309**
	PEG average M_n 2,000 PEI average M_n 30,000		**929867**
PEI Prime(TM) linear polyethylenimine		suitable for gene delivery	**919012**
Poly(ethylene glycol)-block-polyethyleneimine	PEG M_n 750 PEI M_n 15k		**910791**
Poly(ethyleneimine) solution	average M_n 1,200 average M_w 1300	50 wt. % in H2O	**482595**
	average M_n 1,800 average M_w 2,000	50 wt. % in H2O	**408700**
	average M_n 60,000 average M_w 750,000	50 wt. % in H2O	**181978**
Polyethylenimine hydrochloride	average M_n 4,000, PDI ≤1.3	linear	**764892**
	average M_n 10,000, PDI ≤1.5	linear	**764647**
	average M_n 20,000, PDI ≤1.4	linear	**764965**
Polyethylenimine	average M_n 600 average M_w 800	branched	**408719**
	average M_n 10,000 average M_w 25,000	branched	**408727**
	average M_n 10,000, PDI <=1.3	linear	**765090**
	average M_n 2,100, PDI <1.3	linear	**764604**
	average M_n 5,000, PDI <=1.3	linear	**764582**

Product Highlight

Formulation Made Easier

NanoFabTx™ Formulation Kits

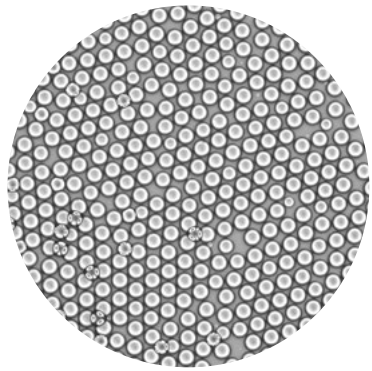

Formulate faster with our ready-to-use NanoFabTx™ formulation kits.

NanoFabTx™ kits facilitate early-stage drug nanoformulation screening with optimized protocols and a curated selection of polymer-based materials for reproducible synthesis of nano- to micro-sized particles for drug encapsulation.

Key Features:

- Step-by-step protocols
- Create uniform and reproducible nanoparticles
- Optimized to make nanoparticles by nanoprecipitation or microfluidics
- Based on non-toxic, biodegradable polymers
- Material screening kits available

Sigma-Aldrich.com/nanofabtx

Approaches to the Design of Lipid-based Nanocarriers for mRNA Delivery

Xing Duan, Xiangrong Song*

Department of Critical Care Medicine, Department of Clinical Pharmacy, Frontiers Science Center for Disease-related Molecular Network, State Key Laboratory of Biotherapy and Cancer Center, West China Hospital, Sichuan University, Chengdu, 610041, China.

*Email: songxr@scu.edu.cn

Introduction

A variety of carriers, including lipid-based nanocarriers (LNPs), polymeric nanoparticles, cationic nanoemulsions (CNEs), and other delivery systems, have been synthesized to protect mRNA from degradation by widely present RNase and are crucial to the development of mRNA drugs. LNPs are the most prominent mRNA drug delivery systems due to their high efficiency and low toxicity. Two LNP-based mRNA vaccines, BNT162b2 (from Pfizer BioNTech) and mRNA-1273 (from Moderna), have been approved by the US FDA for controlling the SARS-CoV-2 pandemic.[1] Generally, LNPs are composed of four components: cationic or ionizable lipids, neutral phospholipids, cholesterol, and polyethylene glycol-modified lipids. Cationic lipids were the first used to construct LNP delivery systems and have been widely used to deliver gene medicines, including DNA, siRNA, and plasmids et al. However, its development was restricted by its relatively low efficiency in delivering mRNA and certain toxic side effects. Therefore, correctly utilizing cationic lipids to develop efficient LNPs is a significant scientific problem that urgently needs to be studied.

Ionizable lipids are integral to the safety and efficacy of LNPs, and are crucial in determining mRNA loading, expression, and targeting.[2] For example, the ionizable lipids used in Patisiran, BNT162b2, and mRNA-1273 are DLin-MC3-DMA (MC3), ALC-0315, and SM-102. However, it still needs to be clarified how the chemical structure of ionizable lipids affects the delivery efficiency of LNPs for mRNA. At the same time, developing efficient LNPs requires the meticulous design of formulations and the selection of appropriate routes of administration. Therefore, in this review, we explore how to use cationic lipids properly, develop highly efficient ionizable lipids, conduct innovative research on the prescription of LNPs, and choose the route of LNP administration.

Cationic Lipids for mRNA Delivery

Liposomes are considered the earliest lipid nanoparticles because they are composed of lipids and, in most cases, are nanoscale. Liposomes can effectively improve the water solubility of drugs and help most lipid-soluble drugs enter the clinic, such as doxorubicin liposomes and Epaxal. In nucleic acid drug delivery, cationic liposomes composed of cationic lipids with a constant positive charge can effectively carry negatively charged nucleic acids. Cationic lipids have been broadly used in mRNA delivery, including N-[1-(2,3-dioleoyloxy)propyl]-N,N,N-trimethylammonium chloride (DOTMA), 1,2-dioleoyloxy-3-trimethylammonium propane chloride (DOTAP)[3], 1,2-stearoyl-3-trimethylammonium-propane (DSTAP), and 1,2-dimyristoyl-3-trimethylammonium-propane (DMTAP). Lipid nanoparticles constructed with these cationic lipids and other auxiliary materials can effectively deliver nucleic acid drugs within the body. However, with the emergence of ionizable lipids, nucleic acid delivery systems based on ionizable lipids show more efficient delivery performance than those based on cationic lipids. Therefore, the development of cationic lipids has entered a bottleneck period.

Selective Organ Targeting (SORT) Delivery System

Fortunately, researchers have found an effective way to use cationic lipids, the most prominent of which is the selective organ targeting (SORT) delivery theory. Cheng et al. replaced some auxiliary lipids with cationic lipids to construct an mRNA delivery

system with a specific organ-targeting function. Adding cationic lipids could effectively regulate the zeta potential of LNPs and the type of protein adsorbed by LNPs during transport in the body, thus realizing organoselective LNPs (Figure 1).[4]

Surface Modification and Functionalization of Cationic Liposomes

On the other hand, highly positively charged cationic nanovaccines may destroy blood cells and cause hemolysis. At the same time, they will be cleared by the reticuloendothelial system due to the absorption of excessive serum proteins, resulting in low efficiency of mRNA delivery in the body. To overcome this challenge, Song et al. prepared negatively charged mRNA vaccines by modifying natural anionic polymers onto the surface of cationic liposomes. This strategy effectively reduced the toxicity of cationic liposomes and achieved efficient mRNA delivery. Sodium alginate, hyaluronic acid, Dex-Aco, and other anionic polymers have been used to modify cationic liposomes, and this anionic coating strategy may have unique advantages in the development of cationic liposomes (Figure 2).[5]

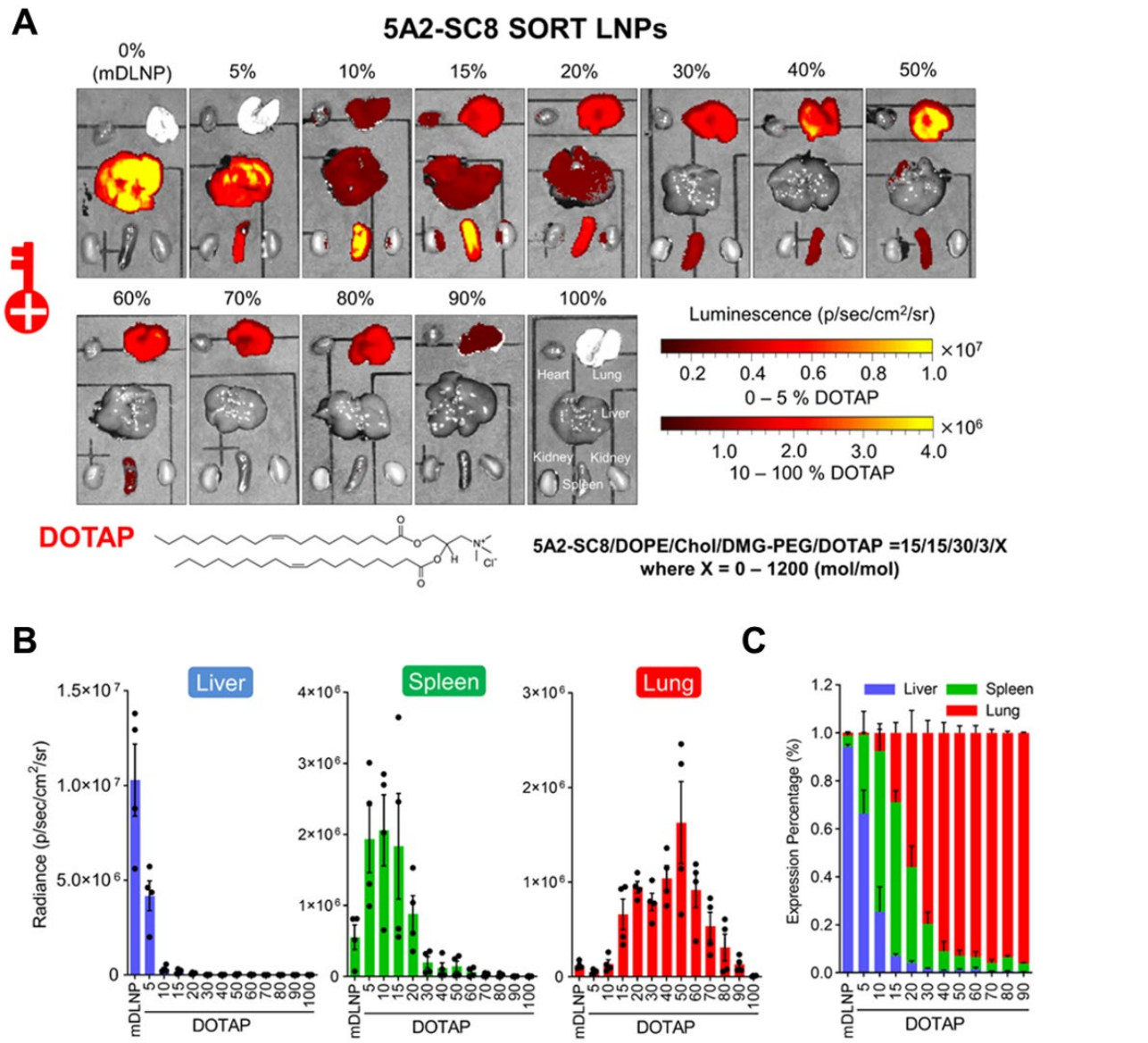

Figure 1. Selective Organ Targeting (SORT) allows lipid nanoparticles (LNPs) to be systematically and predictably engineered to deliver mRNA into specific organs accurately. A) 5A2-SC8 SORT LNPs were formulated as indicated to make a series of LNPs with 0% to 100% SORT lipid (fraction of total lipids). Here, inclusion of a permanently cationic lipid (DOTAP) systematically shifted luciferase protein expression from the liver to spleen to lung as a function of DOTAP percentage. B) Quantification data demonstrated that SORT molecule percentage is the most crucial factor for tissue-specific delivery. Data were shown as mean±s.e.m. (n=4 biologically independent animals). C) Relative luciferase expression in each organ demonstrated that fractional expression could be predictably tuned (0.1 mg/kg Luc mRNA, IV, 6h). Data are shown as mean±s.e.m. (n=4 biologically independent animals). Reprinted with permission from reference 4, copyright 2020 Springer Nature.

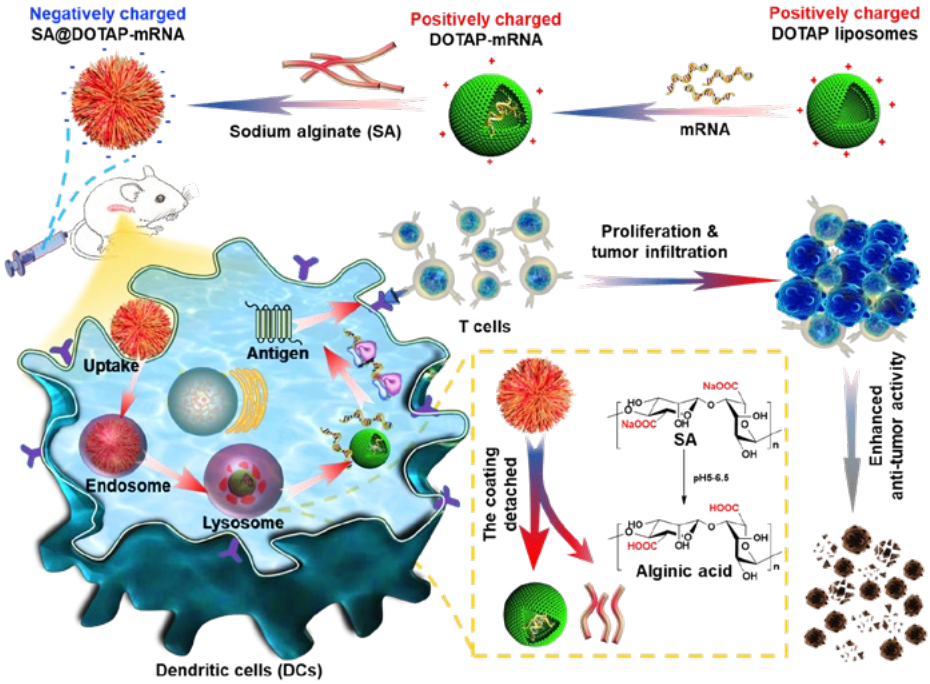

Figure 2. Negatively charged SA@DOTAP-mRNA was prepared by coating DOTAP-mRNA liposomes with SA, which contributed to the lysosome escape of the liposome/mRNA complex and induced a stronger immune response. Reprinted with permission from reference 5, copyright 2022 Elsevier.

Ionizable Lipids for mRNA Delivery

LNPs based on ionizable lipids have achieved promising therapeutic effects in clinical practice, and ionizable lipids, the core component of LNPs, play a decisive role in loading mRNA, protecting mRNA from RNase degradation, and controlling mRNA release. Clinically, the earliest ionizable lipid used to deliver nucleic acids was Dlin-MC3-DMA (MC3), which has been used to deliver siRNA clinically for treating transthyretin-mediated amyloidosis. In 2022, ionizable lipids ALC-0315 (Pfizer) and SM-102 (Moderna) were utilized in COVID-19 vaccine nanoparticles, becoming the only two mRNA vaccines in the world to be approved by the FDA for use against SARS-CoV-2. Currently, various mRNA drugs based on ionizable lipids are under clinical study.

The chemical structure of ionizable lipids plays a crucial role in nucleic acid delivery, so many preclinical studies have been conducted to reveal the effect of their chemical structure on nucleic acid delivery. Ionizable lipids are amphiphilic molecules that contain three domains: a polar head group, a hydrophobic tail region, and a linker between the two domains.

Polar Head Group of Ionizable Lipids

The head is composed of one or more protonatable N atoms. Although the three lipids currently on the market all contain only one protonatable N atom, it is unclear whether ionizable lipids whose heads contain a specific number of protonatable N atoms are more suitable for nucleic acid delivery. Song et al. designed a library of ionizable lipid compounds with a 4N4T structure. 4N4T ionizable lipids can be divided into hydrophilic centers and hydrophobic tails. The hydrophilic center consists of four tertiary amines (N) and four saturated hydrophobic chains (T). These 4N4T LNPs exhibit much higher mRNA translation efficiency than the approved SM 102 LNPs, and these 4N4T-based COVID-19 mRNA vaccines successfully trigger robust and durable humoral immune responses against SARS-CoV-2 and its variants, including Delta and Omicron. Importantly, 4N4T-based COVID-19 mRNA vaccines have higher RBD-specific IgG titers and neutralizing antibody titers than mRNA vaccines based on SM 102.[6] Other ionizing lipids based on multi-N atoms include C12-200, 5A2-SC8, 306Oi10, TT3, and C14-4.[7] Although, according to the literature data, these carriers have not been compared head-to-head with SM102 or ALC-0315, they may have the same mRNA delivery capacity as SM102 and ALC0315.

The Hydrophobic Tail Region of Ionizable Lipids

Dan Peer et al. developed a series of ionizable lipids with different tail structures based on the same head. They found that lipids with a branched chain and ester bonds were less effective than those with linoleic fatty acid chains. This could be attributed to a better endosomal escape due to the structural change of linoleic lipids.[8] In another study, a small library of lipoids using 3,3′-diamino-N-methyldipropylamine was designed to react with 11 saturated alkyl acrylate tails varying in length from 6 to 18. Results found that the lipoid 306Oi10 with a one-carbon branch in the tail conferred a tenfold improvement over the lipoid 306O10 with a straight tail. Nanoparticles containing 306Oi10 ionize at endosomal pH 5.0, thereby improving mRNA delivery.[9]

Linker between the polar head group and hydrophobic tail

The head and tail ligand structure of ionized lipids plays an essential role in controlling the stability of LNPs, organ targeting during transport *in vivo*, and the release rate of nucleic acid molecules. Virgil Percec et al. found that LNPs had more obvious targeting in the liver and spleen when the ligand structure was an ester bond and more specific lung targeting when the ligand structure was an amide bond.[10] This was also confirmed by the research work of Qiaobing Xu et al. By comparing 306Oi10 series ionizable lipids with 306N12B ionizable lipids, we can be better convinced that the linking groups play a prominent role in regulating the organ selectivity of LNPs.[11] In addition, biodegradable lipids can also be made of both ester and disulfide motifs. Cleavage of the disulfide bonds drives an intraparticle nucleophilic attack on the ester linker, accelerating their degradation.[12]

Although the three components of ionizable lipids have their roles, the whole is greater than the local addition. In developing efficient ionizable lipids, we should design from the perspective of the whole molecule and choose the appropriate combination.

Research and Development of Highly Efficient Ionizable Lipids

Ionizable lipids are the core components of LNPs, so their development has attracted much attention. According to the review in Nature Communications, ionizable lipids are divided into five categories. Unsaturated ionizable lipids (DLin-MC3-DMA, A6, OF-O2, A18-Iso5-2DC18), multi-tail ionizable lipids (98N12-5, C12-200, 9A1P9 and cKK-E12), ionizable polymer-lipids (7C1 and G0-C14), biodegradable ionizable lipids (L319, 304O13, OF-Deg-Lin, 306-O12B) and branched-tail ionizable lipids (306Oi10, FTT). Based on current research progress and clinical status, degradable backbones and increased branching/tails are two of the most favorable structural properties for the future development of ionizable lipids. SM-102 and ALC-0315 have shared features, including a tertiary amine, branched tails, and ester linkers. Moreover, both exhibit extended aliphatic branches, making them resemble multi-tail structures. In addition to safety and potency, next-generation ionizable lipids with additional functions, such as targeting and immune regulation, will play an important role in specific applications. Currently, more than half of the LNPs are

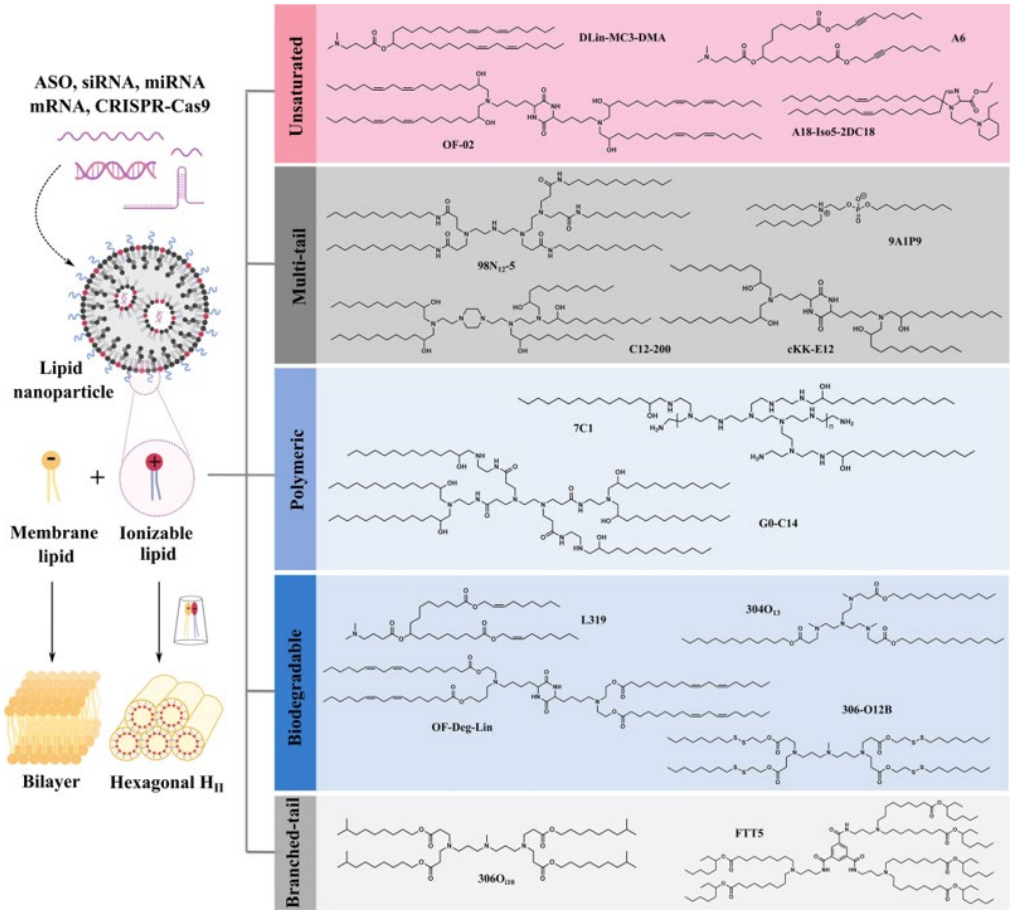

Figure 3. The cone-shaped ion pairs formed by anionic endosomal phospholipids and protonated ionizable lipids can disrupt the bilayer structure to promote endosomal escape. Based on their structural properties, RNA-delivering ionizable lipids can be categorized into unsaturated (containing unsaturated bonds), multi-tail (containing more than two tails), polymeric (containing polymer or dendrimer), biodegradable (containing biodegradable bonds) and branched-tail (containing branched tail) ones. Reprinted with permission from reference 13, copyright 2021 Springer Nature.

ionizable lipids targeted to the liver, spleen, lung, heart, kidney, pancreas, and other organs. There are still huge opportunities for innovation to realize the broader application prospects of RNA therapy.[13]

Prescription Design of LNPs

The formulations of commercially available LNPs are very similar. The formulations of LNPs consist of 35%-50% ionizable lipids, and the remaining 10%-20% are neutral lipids, 35-40% cholesterol, and 0.5%-2.5% PEG. In addition to ionizable lipids, other innovations are possible, such as replacing cholesterol with ß-sitosterol. ß-Sitosterol gives LNPs a polyhedral shape, which is conducive to endosome escape. The optimized LNPs showed uniform particle distribution, polyhedral morphology, and rapid stretched diffusion, which enhanced gene transfection.[14] In addition, neutral phospholipids are replaced by cationic or anionic phospholipids to regulate the zeta potential of LNPs and achieve organ-selective delivery of LNPs.[15] Other types of phospholipids and PGE are also being developed to improve the delivery capacity of LNPs. **Figure 4** shows representative structures of LPN components.

Administration Route of LNPs

Different modes of administration of LNPs will significantly affect the distribution of LNPs in organs, mRNA expression duration, and the types of cells that ingest LNPs, thus leading to different therapeutic effects. Intravenous and intramuscular injections of LNPs have been clinically applied, while other modes of administration are still under clinical and preclinical study. Yuhong Xu et al. injected LNPs through intramuscular, subcutaneous, and intravenous routes, and the results showed that LNPs in intravenous injection mainly accumulated in the liver, and the expression of luciferase in the liver peaked at 4 h and rapidly decreased within 48 h. LNPs injected intramuscularly may reside at the injection site, but gene expression is also evident in the liver. LNPs injected subcutaneously resided at the injection site and produced weaker mRNA expression.[16] Kathryn A. Whitehead et al. selected 396Oi10, 200Oi10, and 514Oi10 to prepare three LNPs. Compared with intravenous injection (IV), intra-abdominal injection (IP) significantly enhanced the effectiveness and specificity of mRNA-targeted pancreatic delivery and helped to improve delivery and specificity.[17] Also, based on the elaborate design of prescriptions, James E. Dahlman et al. constructed an LNP called Nebulized Lung Delivery 1 (NLD1) for further analysis. By comparing the relative sizes of different DLS peaks, the researchers found that NLD1 was more stable than 7C3, cKK-E12, and MC3 after nebulization. Finally, NLD1 was stable and well tolerated after nebulization, and the lung transfection efficiency was higher.[18] Other drug delivery routes have also been used for LNP delivery. Niren Murthy et al. delivered LNPs into fetal mice by intrauterine injection and achieved effective transfection in the liver, heart, kidney, lung, gastrointestinal tract, and brain, with transfection levels exceeding 5%. This strategy is promising for the prevention and treatment of a variety of fetal diseases.[19]

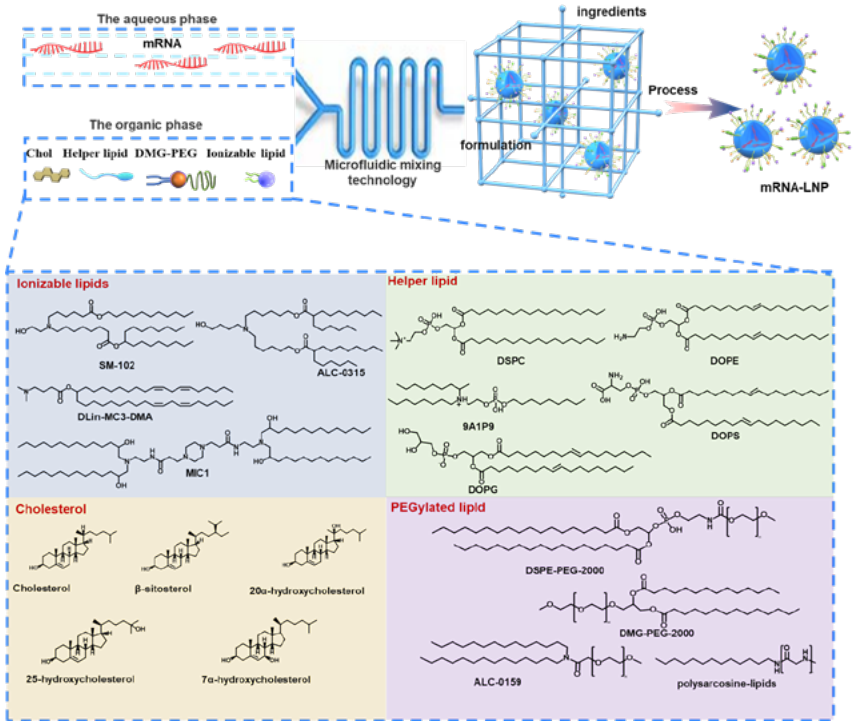

Figure 4. Representative structures of LNP components. LNP composition, prescription ratio, and preparation technology all have a crucial influence on the effect of LNPs. LNPs usually contain four components, namely, ionizable cationic lipids, phospholipids, cholesterol, and PEGylated lipids. They can self-assemble into nanosized LNPs via the ethanol dilution method. Here, representative compounds for each component are listed.

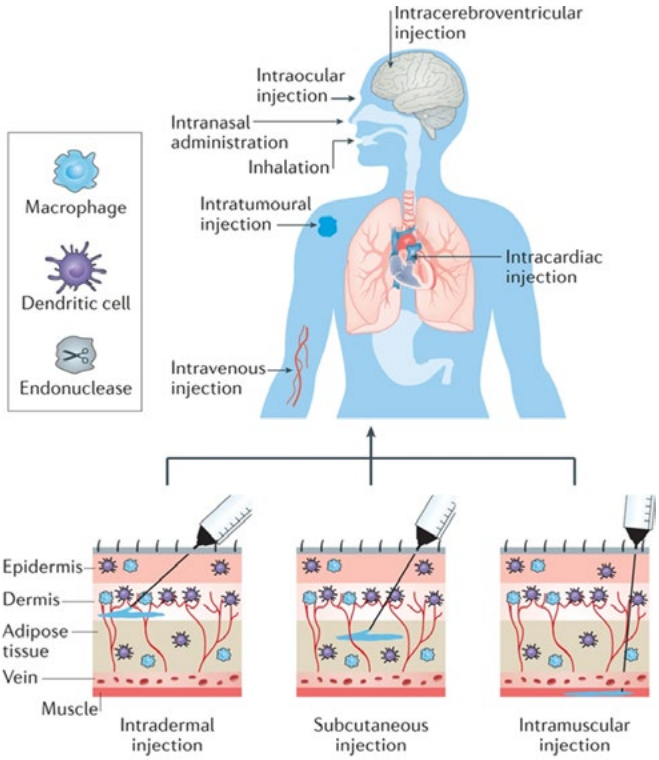

Figure 5. Administration routes for LNP-mRNA formulations. LNPs can be treated by intravenous injection, intramuscular injection, subcutaneous injection, intradermal injection, and aspiration administration. Copyright Springer Nature Limited.

Perspective

In the past decade, the development of LNPs has grown significantly. Currently, there are three commercially available LNPs and several clinical and preclinical studies related to LNPs. An increasing number of LNPs are expected to enter the market in the next few years. This paper summarizes the status quo of LNPs in recent years and some essential key points to guide future LNP research and development.

First, efficient delivery vectors are the key to the success of LNPs. Although cationic lipids may not be as good as ionizable lipids for mRNA delivery, they should not be abandoned. Surface modification, prescription optimization, and strategies of mixing with ionizable lipids may contribute to the development of cationic lipids. Second, when developing new lipid molecules, the three components of lipids should be taken into full consideration, and the chemical structure of the carrier should be adjusted for research and development to design an efficient, safe, and organ-selective carrier. Third, the design of prescriptions and the choice of administration route are also significant in the research and development of LNPs. Many auxiliary compounds may improve the stability of LNPs and the delivery efficiency of LNPs to mRNA. At the same time, the administration route of LNPs also has a crucial impact on their efficacy. Adjusting the prescription of LNPs must be addressed, as LNPs face different delivery barriers under different delivery routes.

Finally, each part of LNP research and development is essential, and the whole is greater than the sum of the parts. Researchers should properly design the chemical structure of the delivery vector, fine-tune the prescription composition of LNPs, and select the appropriate route of administration according to their own research and development purposes.

Acknowledgments

This study was supported by the National Key Research and Development Program of China (2021YFE0206600), the Sichuan Province Science and Technology Support Program (2021YFSY0008 and 2020YJ0238), the Translational Medicine Fund of West China Hospital (CGZH19002) and the 1.3.5 Project for Disciplines of excellence, West China Hospital, Sichuan University (ZYGD18020/ZYJC18006).

References

(1) Regev-Yochay, G.; et al. *N. Engl. J. Med.* **2022**, *386* (14), 1377–1380. DOI:10.1056/NEJMc2202542
(2) Chaudhary, N.; Weissman, D.; Whitehead, K. A. *Nat. Rev.* **2021**, *20* (11), 817–838. DOI:10.1038/s41573-021-00283-5
(3) LoPresti, S. T.; Arral, M. L.; Chaudhary, N.; Whitehead, K. A. *J. Control. Release* **2022**, *345*, 819–831. DOI:10.1016/j.jconrel.2022.03.046
(4) Cheng, Q.; Wei, T.; Farbiak, L.; Johnson, L. T.; Dilliard, S. A.; Siegwart, D. J. *Nat. Nanotechnol.* **2020**, *15* (4), 313–320. DOI:10.1038/s41565-020-0669-6
(5) Duan, X.; Zhang, Y.; et al. *Acta Pharm. Sin. B* **2023**, *13* (3), 942–954. DOI:10.1016/j.apsb.2022.08.015
(6) Chen, K.; Fan, N.; Huang, H.; Jiang, X.; et al. *Adv. Funct. Mater.* **2022**, *32* (39), 2204692. DOI:10.1002/adfm.202204692
(7) Qin, S.; Tang, X.; et al. *Signal Transduct. Target. Ther.* **2022**, *7* (1), 166. DOI:10.1038/s41392-022-01007-w
(8) Elia, U.; et al. *ACS Nano* **2021**, *15* (6), 9627–9637. DOI:10.1021/acsnano.0c10180
(9) Hajj, K. A.; et al. *Small* **2019**, *15* (6), e1805097. DOI:10.1002/smll.201805097
(10) Zhang, D.; et al. *J. Am. Chem. Soc.* **2021**, *143* (43), 17975–17982. DOI:10.1021/jacs.1c09585

(11) Qiu, M.; Tang, Y.; Chen, J.; Muriph, R.; Ye, Z.; Huang, C.; Evans, J.; Henske, E. P.; Xu, Q. *Proc. Natl. Acad. Sci. U. S. A.* **2022**, *119* (8). DOI:10.1073/pnas.2116271119
(12) Hou, X.; Zaks, T.; Langer, R.; Dong, Y. *Nat. Rev. Mater.* **2021**, *6* (12), 1078–1094. DOI:10.1038/s41578-021-00358-0
(13) Han, X.; Zhang, H.; Butowska, K.; Swingle, K. L.; Alameh, M. G. *Nat. Commun.* **2021**, *12* (1), 7233. DOI:10.1038/s41467-021-27493-0
(14) Kim, J.; Jozic, A.; Lin, Y.; Eygeris, Y.; Bloom, E.; Tan, X.; Acosta, C.; MacDonald, K. D.; Welsher, K. D.; Sahay, G. *ACS Nano* **2022**, *16* (9), 14792–14806. DOI:10.1021/acsnano.2c05647
(15) Wang, X.; Liu, S.; et al. *Nat. Protoc.* **2023**, *18* (1), 265–291. DOI:10.1038/s41596-022-00755-x
(16) Di, J.; et al. *Pharm. Res.* **2022**, *39* (1), 105–114. DOI:10.1007/s11095-022-03166-5
(17) Melamed, J. R.; et al. *Sci. Adv.* **2023**, *9* (4), eade1444. DOI:10.1126/sciadv.ade1444
(18) Lokugamage, M. P.; Vanover, D.; et al. *Nat. Biomed. Eng.* **2021**, *5* (9), 1059–1068. DOI:10.1038/s41551-021-00786-x
(19) Gao, K.; et al. *Bioact. Mater.* **2023**, *25*, 387–398. DOI:10.1016/j.bioactmat.2023.02.011

NanoFabTx™ Drug Delivery Formulations

NanoFabTx™ Lipid Mixes

Name	Description	Cat. No.
NanoFabTx™ - COOH Lipid Mix	for synthesis of carboxyl functionalized liposomes	**930113**
NanoFabTX™ - DOTAP Lipid Mix	for synthesis of cationic (DOTAP) liposomes	**926027**
NanoFabTX™ - NH2 Lipid Mix	for synthesis of amine functionalized liposomes	**924512**
NanoFabTx™ - PEG Lipid Mix	for synthesis of PEGylated liposomes	**922420**
NanoFabTx™- DC-Chol Lipid Mix	for synthesis of cationic (DC-cholesterol) liposomes	**926345**

NanoFabTx Device Kits

Name	Description	Cat. No.
NanoFabTx™ microfluidic - micro	device kit for synthesis of 10-30 µm particles	**911879**
	device kit for synthesis of 1-5 µm particles	**911860**
NanoFabTx™ microfluidic - nano	device kit for synthesis of 100-200 nm nanoparticles and liposomes	**911593**

Preformulated Liposomes

Cationic Liposomes

Description	DOTAP:DOPC Ratio	Size	Cat. No.
DOTAP-based, phosphate buffered saline	50:50	100 nm	**CDP-501**
	40:60	100 nm	**CDP-502**
	30:70	100 nm	**CDP-503**
	20:80	100 nm	**CDP-504**
	10:90	100 nm	**CDP-505**
	5:95	100 nm	**CDP-506**
	2:98	100 nm	**CDP-507**
	1:99	100 nm	**CDP-508**
	0.5:99.5	100 nm	**CDP-509**

Cationic Liposomes for DNA/RNA delivery

Description	Concentration	Contains	Cat. No.
DOTAP:Cholesterol, deionized RNAse-free water	2 mM DOTAP 2 mM Cholesterol		**GEN-7001**
DOTAP:DOPE, deionized RNAse-free water	2 mM DOTAP 2 mM DOPE		**GEN-7002**
DOTAP:Cholesterol, deionized RNAse-free water	2 mM DOTAP 2 mM Cholesterol	0.02 mM NBD-DOPE as fluorescent label	**GEN-7003**
DOTAP:Cholesterol, deionized RNAse-free water	2 mM DOTAP 2 mM Cholesterol	0.02 mM Rhod-PE as fluorescent label	**GEN-7004**
DOTAP:DOPE, deionized RNAse-free water	2 mM DOTAP 2 mM DOPE	0.02 mM NBD-DOPE as fluorescent label	**GEN-7005**
DOTAP:DOPE, deionized RNAse-free water	2 mM DOTAP 2 mM DOPE	0.02 mM Rhod-PE as fluorescent label	**GEN-7006**
DOTAP, deionized RNAse-free water	2 mM DOTAP	0.002 mM DiO as fluorescent label	**GEN-7007**
DOTAP, deionized RNAse-free water	2 mM DOTAP	0.002 mM DiI as fluorescent label	**GEN-7008**
DDAB:Cholesterol, deionized RNAse-free water	2 mM DDAB 2 mM Cholesterol		**GEN-7009**
DDAB:DOPE, deionized RNAse-free water	2 mM DDAB 2 mM DOPE		**GEN-7010**
DDAB, deionized RNAse-free water	2 mM DDAB		**GEN-7011**
DDAB:Cholesterol, deionized RNAse-free water	2 mM DDAB 2 mM Cholesterol	0.02 mM NBD-DOPE as fluorescent label	**GEN-7012**
DDAB:Cholesterol, deionized RNAse-free water	2 mM DDAB 2 mM Cholesterol	0.02 mM Rhod-PE as fluorescent label	**GEN-7013**
DDAB:DOPE, deionized RNAse-free water	2 mM DDAB 2 mM DOPE	0.02 mM NBD-DOPE as fluorescent label	**GEN-7014**
DDAB:DOPE, deionized RNAse-free water	2 mM DDAB 2 mM DOPE	0.02 mM Rhod-PE as fluorescent label	**GEN-7015**
DDAB, deionized RNAse-free water	2 mM DDAB	0.02 mM NBD-DOPE as fluorescent label	**GEN-7016**
DDAB, deionized RNAse-free water	2 mM DDAB	0.02 mM Rhod-PE as fluorescent label	**GEN-7017**
DOTMA:Cholesterol, deionized RNAse-free water	2 mM DOTMA 2 mM Cholesterol		**GEN-7018**
DOTMA:DOPE, deionized RNAse-free water	2 mM DOTMA 2 mM DOPE		**GEN-7019**
DOTMA, deionized RNAse-free water	2 mM DOTMA		**GEN-7020**
DOTMA:Cholesterol, deionized RNAse-free water	2 mM DOTMA 2 mM Cholesterol	0.02 mM NBD-DOPE as fluorescent label	**GEN-7021**
DOTMA:Cholesterol, deionized RNAse-free water	2 mM DOTMA 2 mM Cholesterol	0.02 mM Rhod-PE as fluorescent label	**GEN-7022**
DOTMA:DOPE, deionized RNAse-free water	2 mM DOTMA 2 mM DOPE	0.02 mM NBD-DOPE as fluorescent label	**GEN-7023**
DOTMA:DOPE, deionized RNAse-free water	2 mM DOTMA 2 mM DOPE	0.02 mM Rhod-PE as fluorescent label	**GEN-7024**
DOTMA, deionized RNAse-free water	2 mM DOTMA	0.002 mM DiO as fluorescent label	**GEN-7025**
DOTMA, deionized RNAse-free water	2 mM DOTMA	0.002 mM DiI as fluorescent label	**GEN-7026**
DC-Cholesterol:DOPE, deionized RNAse-free water	2 mM DC-Cholesterol 2 mM DOPE		**GEN-7027**
DC-Cholesterol:DOPE, deionized RNAse-free water	2 mM DC-Cholesterol 4.01 mM DOPE		**GEN-7028**
DC-Cholesterol:DOPE, deionized RNAse-free water	2 mM DC-Cholesterol 2 mM DOPE	0.02 mM NBD-DOPE as fluorescent label	**GEN-7029**
DC-Cholesterol:DOPE, deionized RNAse-free water	2 mM DC-Cholesterol 2 mM DOPE	0.02 mM Rhod-PE as fluorescent label	**GEN-7030**
DC-Cholesterol:DOPE, deionized RNAse-free water	2 mM DC-Cholesterol 3.98 mM DOPE	0.02 mM NBD-DOPE as fluorescent label	**GEN-7031**
DC-Cholesterol:DOPE, deionized RNAse-free water	2 mM DC-Cholesterol 3.98 mM DOPE	0.02 mM Rhod-PE as fluorescent label	**GEN-7032**
GL-67:DOPE, deionized RNAse-free water	2 mM GL-67 4.01 mM DOPE		**GEN-7033**
GL-67:DOPE, deionized RNAse-free water	2 mM GL-67 3.98 mM DOPE	0.03 mM NBD-DOPE as fluorescent label	**GEN-7034**
GL-67:DOPE, deionized RNAse-free water	2 mM GL-67 3.98 mM DOPE	0.03 mM Rhod-PE as fluorescent label	**GEN-7035**

Anionic Liposomes

Description	Ratio	Size	Cat. No.
Phosphatidylglycerol (PG)-based, phosphate buffered saline	90 mol % DOPG 10 mol % DOPC	100 nm	**CPG-501**
	80 mol % DOPG 20 mol % DOPC	100 nm	**CPG-502**
	70 mol % DOPG 30 mol % DOPC	100 nm	**CPG-503**
	60 mol % DOPG 40 mol % DOPC	100 nm	**CPG-504**
	50 mol % DOPG 50 mol % DOPC	100 nm	**CPG-505**
	40 mol % DOPG 60 mol % DOPC	100 nm	**CPG-506**
	30 mol % DOPG 70 mol % DOPC	100 nm	**CPG-507**
	20 mol % DOPG 80 mol % DOPC	100 nm	**CPG-508**
	10 mol % DOPG 90 mol % DOPC	100 nm	**CPG-509**
	5 mol % DOPG 95 mol % DOPC	100 nm	**CPG-510**
	2 mol % DOPG 98 mol % DOPC	100 nm	**CPG-511**
	1 mol % DOPG 99 mol % DOPC	100 nm	**CPG-512**
	0.5 mol % DOPG 99.5 mol % DOPC	100 nm	**CPG-513**
	100 mol % DOPG	100 nm	**CPG-514**
Phosphatidylserine (PS)-based, phosphate buffered saline	10 mol % DOPC 90 mol % DOPS	100 nm	**CPS-501**
	20 mol % DOPC 80 mol % DOPS	100 nm	**CPS-502**
	30 mol % DOPC 70 mol % DOPS	100 nm	**CPS-503**
	40 mol % DOPC 60 mol % DOPS	100 nm	**CPS-504**
	50 mol % DOPC 50 mol % DOPS	100 nm	**CPS-505**
	60 mol % DOPC 40 mol % DOPS	100 nm	**CPS-506**
	70 mol % DOPC 30 mol % DOPS	100 nm	**CPS-507**
	80 mol % DOPC 20 mol % DOPS	100 nm	**CPS-508**
	90 mol % DOPC 10 mol % DOPS	100 nm	**CPS-509**
	95 mol % DOPC 5 mol % DOPS	100 nm	**CPS-510**
	98 mol % DOPC 2 mol % DOPS	100 nm	**CPS-511**
	99 mol % DOPC 1 mol % DOPS	100 nm	**CPS-512**
	99.5 mol % DOPC 0.5 mol % DOPS	100 nm	**CPS-513**
	100 mol % DOPS	100 nm	**CPS-514**

PEGylated Liposomes

Name	Description	Ratio	Cat. No.
Neutral PEGylated Liposomes	HSPC:Chol:DSPE-PEG(2000)	65 mol % HSPC 30 mol % Cholesterol 5 mol % DSPE-PEG2000	**CPCG-501**
	DSPC:Chol:DSPE-PEG(2000)	65 mol % DSPC 30 mol % Cholesterol 5 mol % DSPE-PEG2000	**CPCG-502**
	DOPC:Chol:DOPE-PEG(2000)	65 mol % DOPC 30 mol % Cholesterol 5 mol % DSPE-PEG2000	**CPCG-503**
Anionic PEGylated Liposomes	DSPC:Chol:DSPS:DSPE-PEG(2000)	60 mol % DSPC 30 mol % Cholesterol 5 mol % DSPS 5 mol % DSPE-PEG2000	**CPSG-501**
	DOPC:Chol:DOPS:DOPE-PEG(2000)	60 mol % DOPC 30 mol % Cholesterol 5 mol % DOPS 5 mol % DOPE-PEG2000	**CPSG-502**
Cationic PEGylated Liposomes	DSPC:Chol:DSTAP:DSPE-PEG(2000)	55 mol % DSPC 30 mol % Cholesterol 10 mol % DSTAP 5 mol % DSPE-PEG2000	**CDPG-501**
	DOPC:Chol:DOTAP:DOPE-PEG(2000)	55 mol % DOPC 30 mol % Cholesterol 10 mol % DOTAP 5 mol % DOPE-PEG2000	**CDPG-502**

The Future of Drug Delivery

Ready-to-use preformulated liposomes

Liposomes are one of the most common drug delivery carriers for small molecules and nucleic acid therapeutics.

We offer a variety of preformulated liposomes including:

- Cationic liposomes
- Natural liposomes
- PEGylate liposomes

Available lyophilized or in solution.

For a complete list of preformulated lyophilized liposomes visit:
SigmaAldrich.com/liposomes

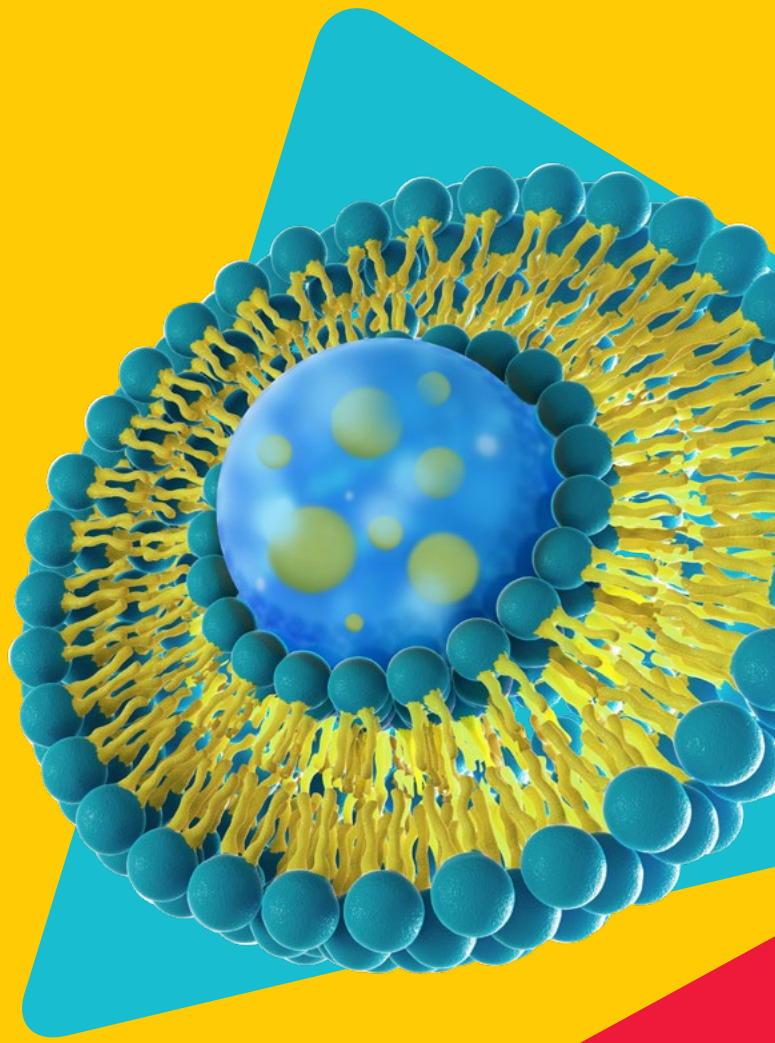

Sigma-Aldrich®
Lab & Production Materials

Recent Advances in 3D-Bioprinting-based Drug Screening: A Mini Review and Perspective



Long He,[1] Yong Luo,[1] Xiuli Zhang[2]*

[1]State Key Laboratory of Fine Chemicals, Department of Pharmaceutical Sciences, School of Chemical Engineering, Dalian University of Technology, 116024, Dalian, Liaoning Province, China

[2]Jiangsu Key Laboratory of Neuropsychiatric Disease and College of Pharmaceutical Science, Soochow University, 215127, Suzhou, Jiangsu Province, China

*Email: zhangxl@suda.edu.cn

Introduction

Three-dimensional culture[1] is becoming an increasingly accepted paradigm for cell cultivation due to its ability to simulate the *in vivo* microenvironment of cells in three dimensions. This fosters better cell viability, particularly for primary cells, and is easy to standardize.[2] It is currently a significant focus for the FDA. Three-dimensional (3D) culture can be divided into suspended 3D culture[3] and scaffold-based 3D culture.[4] The latter is a hot research topic, focusing on developing advanced biomaterials. By embedding cells within such materials, phenotypes can be more apparent, and the cells' functions can be more robust.[5]

Biomaterials can be designed to be printable.[6] 3D bioprinting technologies can customize the shape and internal structure of such materials, as well as precisely 3D position the cells in the materials, thereby achieving highly controllable three-dimensional cell co-culture, which has the potential to simulate tissues and organs.[7] Using 3D bioprinting technology to construct three-dimensional cell co-culture systems is an advanced model for drug screening due to its highly biomimetic nature. This review paper highlights recent progress in 3D bioprinted tissue models and summarizes the advancements of 3D bioprinting in drug discovery. Finally, this paper discusses the future of 3D bioprinting-based drug discovery and how it compares to other biomimetic techniques like organoids[8] and organ chips.[9]

3D Bioprinted Tissue Models

3D-bioprinting-based drug screening relies on 3D bioprinted tissue models that are rapidly advancing, such as 3D-bioprinted liver. The liver's intricate vascular network is crucial for substance exchange during drug metabolism. A good goal is the development of a vascularized *in vitro* liver model using 3D bioprinting. In a recent study, Kang et al. achieved this by creating a heterogeneous, multicellular, multi-material liver lobule array.[10] The team designed a pre-defined 1 mm structure, encompassing a 150 µm diameter central vein channel, high-density liver cells with embedded endothelial cells, 10 µm resolution micro-nozzles, and an external endothelial lining to form a luminal tube. Using a battery of tests, the researchers evaluated the formation status, structural integrity, mechanical performance, liver function expression, and amiodarone-induced liver toxicity. The bioprinted body yielded ideal results in all tests, indicating its potential as an *in vitro* liver construction model.

In recent years, 3D coaxial printing technology has shown great potential in directly manufacturing injectable hollow structures. In particular, Singh[11] and others have made significant progress by developing a decellularized kidney-derived bioink, that is combined with a mixture of sodium alginate, renal proximal tubule epithelial cells (RPTECs), and human umbilical vein endothelial cells (HUVECs) for bioprinting kidney tubular structures. Using a coaxial nozzle, their bioprinter can simultaneously extrude bioink containing free substances and cells. After crosslinking the shell, the middle part is removed, forming complete single or double-layer tubular structures. The RPTEC and HUVEC tubes have also been successfully transplanted into the peritoneal region of immunodeficient mice and implanted into host kidney tissue. Bioprinting of multi-tubular tissue

structures is a promising strategy; most importantly, it is applied in drug reabsorption and excretion and the replacement of damaged kidneys. Deng et al. introduced a novel strategy for constructing hollow tubular structures. By employing a time-dependent crosslinking approach, they successfully controlled the thickness of the tubular wall. An important advantage of this method is its compatibility with cell seeding, allowing for the replication of various tubular structures relevant in vivo, such as blood vessels, renal tubules, etc.[29]

Faheem Ullah et al. describe the successful synthesis of a novel bioink, PEO-CS-PMMA, used to construct skin tissue structures through 3D bioprinting technology.[12] The bioink was obtained by copolymerization of PEO, chitosan, and PMMA to improve its density, viscosity, and printing ability while maintaining thermal stability. The resulting bioink was highly organized and porous, allowing it to absorb water and release growth factors and bioactive substances to promote healing and recovery.

Ma et al. described a method to cross-link bioinks with Ca^{2+} to obtain gelatin-alginate for a 3D bioprinted hydrogel scaffold with good stability and biocompatibility.[13] The scaffold can mimic the physical microenvironment of dermis and subcutaneous tissue by encapsulating adipose stem cells to promote their proliferation and migration. The unique gradient composite scaffold promotes angiogenic and wound healing effects by enhancing the paracrine secretion of adipose stem cells. This 3D-printed scaffold provides a continuous and unique structure for adipose stem cells to promote skin regeneration and can be expanded to complex tissue injury models.

Lee and colleagues utilized fiber-optic-assisted bioprinting to cross-link methacrylate-based hydrogels (GelMA) and construct biofunctional cell-loaded structures by selecting appropriate photocrosslinking process conditions, such as printing temperature.[14] Their experiment induced C2C12 mouse myoblasts and human adipose stem cells (HASCs) to construct cell-loaded structures for muscle regeneration. Compared to traditional printing processes, the cell-loaded structures showed a higher degree of cellular alignment and myogenic activity. Models constructed using HASC also demonstrated superior muscle regeneration compared to those constructed without topographical cues. However, cellular activity factors like cellular metabolism remain challenging, leading to insufficient oxygen transport in the 3D cellular constructs for muscle tissue regeneration. Hwangbo and colleagues addressed this issue by introducing photosynthetic cyanobacteria *(Alcaligenes longum)* into Gelma bioink. They used *in situ* electronic bioprinting to prepare cell-loaded scaffolds that promote cellular arrangement and muscle formation.[15] They concluded that this approach could be an effective treatment for severe skeletal muscle defects by evaluating the combined effects of bioactive components in bioinks and bioprinting that simultaneously support electronic fields.

Bionic spinal scaffolds, based on 3D bioprinting technology, can effectively mimic the shape and structure of spinal cord tissue, and promote the healing of spinal cord injuries. However, they have yet to be successful in mimicking the biological functions of the spinal cord due to insufficient electrical conductivity. Gao et al. developed a new conductive hydrogel, PEDOT:LS, utilized in a bionic scaffold based on GelMA, hyaluronic acid methacrylate (HAMA), and poly (3,4-ethylene dioxythiophene) to mimic the spinal cord's electrical conductivity.[16] The conductive hydrogels showed similar mechanical properties to natural spinal cord tissue, and neural stem cell (NSC) culture showed high survival rates. Compared to non-conductive scaffolds, the 3D bioprinting-based conductive scaffolds significantly promoted neuronal differentiation of NSCs *in vitro* and improved hind limb motor function recovery in a rat spinal cord complete transection model. Zhang et al. introduced inorganic calcium silicate (CS) nanowires in bioink for innervated bone regeneration through 3D bioprinting technology.[17] They established a model that combines nerve and bone-associated cells printed in an orderly fashion, encapsulated by CS nanowires that enhance long-term viability and proliferation of encapsulated cells and promote osteogenesis and neural differentiation. By introducing inorganic nanomaterials into bioinks and 3D bioprinting technology, this work provides a potential strategy for complex bone tissue regeneration.

The combination of 3D bioprinting technology, fused deposition modeling (FDM) technology, and light-cured additive manufacturing (DIW) has significantly advanced cartilage and bone tissue engineering. Chen et al.[18] prepared a biphasic bone scaffold using alginate-gelatin hydrogel (A-G) as the bioink and poly-caprolactone (PCL) to improve mechanical stability and overall performance. The bone phase of the scaffold was enhanced by integrating hydroxyapatite into the PCL, resulting in improved bioactivity. Notably, the physical and biological evaluation of the scaffold in both the bone and cartilage phases confirmed its sound biological effects in both the short and long term, making it a promising interface material between cartilage and bone.

3D Bioprinting for Drug Screening

Compared to 3D-bioprinting-based tissue models, 3D-bioprinting-based drug screening is still in its infancy. Hong et al.[19] used extrusion-based 3D bioprinting technology to fabricate a gelatin-sodium alginate-based construct embedding MCF-7 cells and observed the auto-aggregation of MCF-7 cells into spheroids. These spheroids were found to be able to maintain their drug-resistant phenotype of CD44 high /CD24 low /ALDH1 high and exhibited higher expression levels of drug resistance markers, such as the GRP78 chaperon and ABCG2 transporter. This superior resistance was proven through camptothecin and paclitaxel.

Li et al. developed a 3D-printed breast cancer model with hydroxyethyl cellulose/alginate/gelatin (HCSG) composite biomaterial.[20] They first demonstrated the potential of 3D bioprinting technology used in a structure–activity relationship study, by investigating the pharmacodynamics of 13 amino acid-based flavone phosphoramidates. Compared to 2D monolayer models, 3D printed models presented different pharmacological activity characteristics (Figure 1).

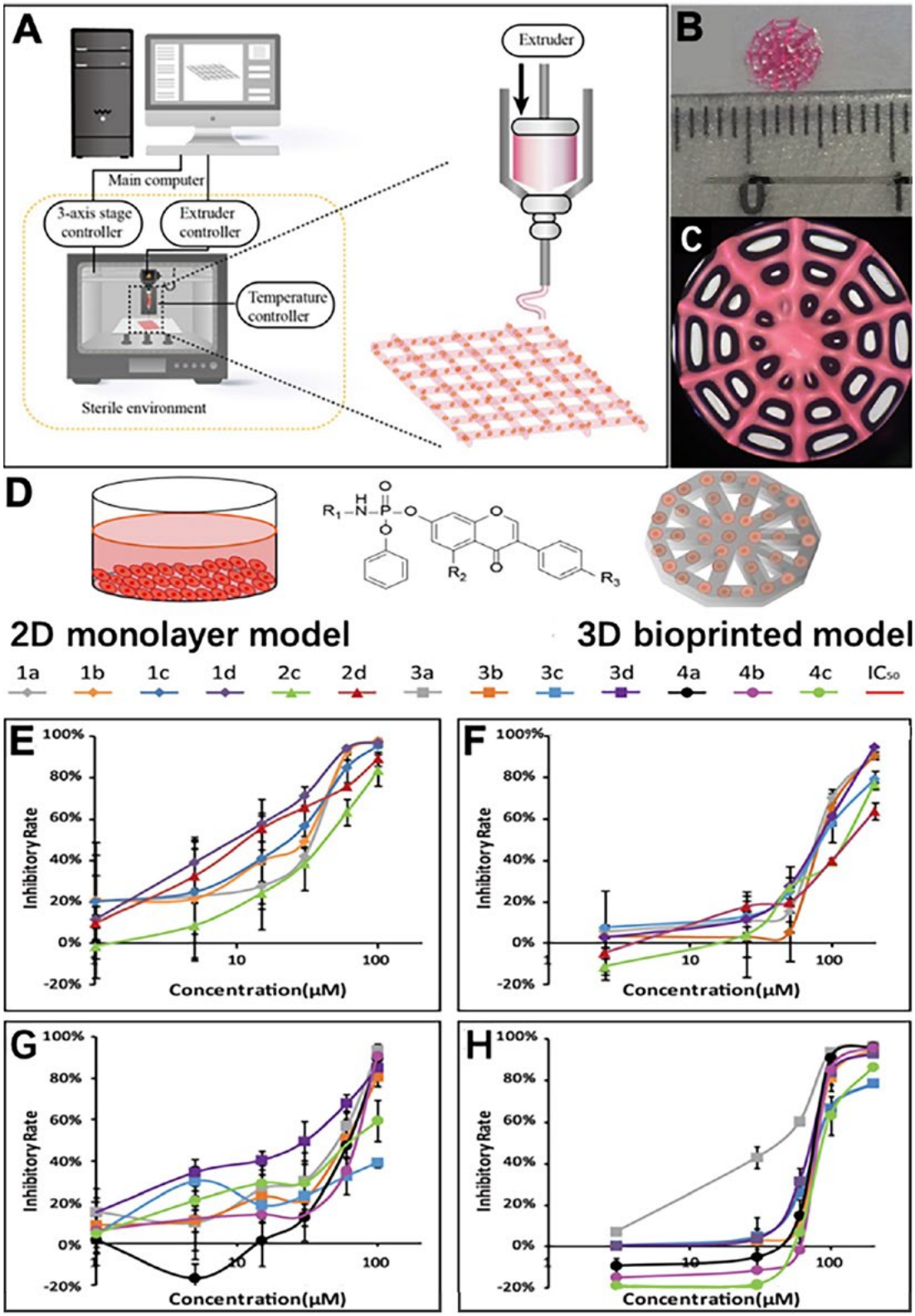

Figure 1. 3D printed breast cancer model. A) Workflow diagram. B–C) Schematic diagram of 3D printed"Spider web" HCSG breast cancer model. D) Investigating pharmacodynamics of 13 amino acid-based flavone phosphoramidates with 2D monolayer model and 3D printed model. Copyright 2020, Zhejiang University Press.

Qiong Liu et al.[21] used sacrificial extrusion-based 3D bioprinting technology to create tubular structures inside the GelMA gel and let cholangiocarcinoma (CCA) cells attach to the surface of the tubular structure to simulate human biliary tract cancer. In this 3D printing model, the authors observed that CCA was overgrowing in a thickening manner, generating bile duct stenosis, which was expected to be analogous to the *in vivo* configuration. Further, CCA cells showed higher sensitivity to anti-tumor drugs than conventional 2D cell models, providing a novel drug screening model for treating bile duct cancer. Decellularized extracellular matrix (DECM) is often added to printable biomaterials to increase biocompatibility.[22]

Janani et al.[23] developed two different bioinks based on tissue specific DECM of liver cells. These bioinks had excellent printability and rheological properties and could support the printing of liver lobules' parenchymal and non-parenchymal cells. The print model showed dose-dependent clinical liver toxicity reactions to acetaminophen and troglitazone, providing a powerful platform for liver toxicity screening. Human-induced pluripotent stem cells (hiPSCs) are a source of cells that can be differentiated into normal human cells.[24] The 3D bioprinting technology can replicate human tissues or organs if normal human cells are used. He Jianyu et al.[25] printed hiPSC-induced-hepatocytes to construct a human liver model. Compared to traditional 2D culture models, hiPSC-induced hepatocytes in this model showed better mRNA expression related to human liver-specific functions and exhibited liver toxicity induced by acetaminophen.

Rency Geevarghese et al. developed a bioink containing several components, including alginate, diethylaminoethylcellulose, gelatin, and collagen peptides, and performed experimental analyses to ensure its suitability for constructing 3D models.[26] The team evaluated the effectiveness of their models by examining the growth and proliferation of A549 cells encapsulated within 3D bioprinted structures. They demonstrated that 3D bioprinting-based tissue models are a more effective means of drug screening, providing a platform that mimics the characteristics of native tissues and offers a superior alternative to current 2D cell toxicity testing. The researchers qualitatively and quantitatively validated the potential of their 3D bioprinted structures as drug screening models using apoptosis assays and MTT assays. In conclusion, their findings suggest that 3D bioprinting has the potential to revolutionize drug screening practices, providing a more effective and reliable means for evaluating drug efficacy.

Zicheng Fan et al. utilized dot extrusion printing (DEP) technology to produce precise positioning and adjustable size of hepatocyte-laden gelatin methacryloyl (GelMA) hydrogel microbeads and HUVEC cell-containing gelatin microbeads, creating endothelialized liver lobule-like structures.[27] Through experimental results, the team found that the appropriate GelMA concentration mimicked the naturally occurring microenvironment and enhanced the growth and propagation of hepatocytes while providing a suitable surface for tight junctions and the growth and proliferation of endothelial cells. Compared to two-dimensional hepatocellular carcinoma cell models, the model obtained through DEP technology also enhanced the efficacy of the antitumor drug sorafenib. The HUVEC-formed endothelial barrier prevented the spread of sorafenib. The authors concluded that DEP technology could potentially construct 3D models of stromal and cancer cells to promote their growth and multiplication, creating a complex tumor microenvironment. The endothelialized hepatocellular carcinoma models based on 3D bioprinted liver lobule-like structures can simulate pharmacodynamics similar to real-life conditions, making them a valuable tool for drug testing.

Xue Liu et al. developed a reproducible method for inducing endothelial cells of different complexity through 3D bioprinting of human keratinocytes, fibroblasts, pericytes, and multifunctional stem cells to fabricate skin models of varying physiological complexity.[28] These included human epidermis, non-vascularized, and vascularized models utilized for high-throughput drug screening on multiwell plates. This innovative combination of 3D cell culture and physiologically relevant 3D tissue models enabled high-throughput pharmacological studies for the first time. The researchers also evaluated the model for the efficacy of potential drugs for AD, with their results correlating with clinical treatment data, highlighting the model's importance in 3D tissue disease modeling and drug screening. Their research offers a valuable tool for future pharmacological studies on multiwell plates and further contributes to 3D tissue disease modeling.

Perspectives

Besides 3D bioprinting, organ-on-a-chip and organoid are two other biomimetic techniques that can be used in drug discovery.

Organ-on-a-chip technology comprises micro-fabricated cell culture systems that accurately mimic the structure, function, and microenvironment of human organs. These microdevices are composed of chambers, microfluidic channels, and sensors that can simulate the complex physiological environment of human organs such as the heart, liver, lung, kidney, and brain. Essentially, the chip mimics the circulation of the blood, the metabolic activities of the cells, and the mechanical forces that act on the organ. Organ-on-a-chip technology has several advantages over traditional cell culture and animal models.

Firstly, it can recreate the complex microenvironments of the organs, including the physical and chemical cues that regulate the growth and function of cells. Secondly, it allows for real-time monitoring and analysis of cellular and molecular changes, enabling researchers to directly observe drug responses and disease progression. Thirdly, it provides a more cost-effective and ethical alternative to animal testing, with the possibility of personalized medicine through patient-derived cells.

Organoids are three-dimensional structures that closely resemble the gross and microscopic anatomy of an organ or tissue. They are formed from self-organizing stem cells that differentiate to

form various cell types found in the desired organ, giving rise to complex functional tissues. Organoids can be created from different types of stem cells, including embryonic stem cells, induced pluripotent stem cells, and adult stem cells. They are valuable tools in drug development, disease modeling, regenerative medicine, and personalized medicine. Organoids have significant advantages over traditional two-dimensional cell cultures and animal models in studying human disease and testing drugs. They provide an accurate representation of the actual organ, including the microenvironment and tissue architecture, allowing for more accurate and reliable drug screening.

Moreover, they minimize the need for animal testing and provide a powerful tool for elucidating the mechanisms of disease progression and novel therapies.

Organoids have been successfully generated from various organs, such as the brain, liver, kidney, pancreas, and intestine, among others. These organoids are being progressively improved by incorporating multiple cell types, establishing vascularization, and introducing functional readouts to approximate organ physiology more closely. With continued advances in stem cell technology and organ engineering techniques, organoids are expected to revolutionize biomedical research and contribute to the development of precision medicine.

3D-bioprinted organs have massive potential in organ transplantation and are perfect alternative models to animal experiments. However, generally, the 3D bioprinted organs are larger in size as compared to organs-on-a-chip and organoids, which limited their use for large-scale screening. The increasing resolution of 3D bioprinting will alleviate this situation. Further, in the future, the 3D bioprinted mini-organ can also be combined with organ-on-a-chip and organoids to develop more biomimetic models for drug discovery.

Acknowledgments

This work was supported by Jiangsu Key Laboratory of Neuropsychiatric Diseases (BM2013003, ZZ2009), the Hunan Key Laboratory for Bioanalysis of Complex Matrix Samples (2017TP1037), Shenzhen Fundamental Research and Discipline Layout project (No. JCYJ2018050815247476), and the National Key Research and Development Program of China (No. 2017YFC1702001).

References

(1) Habanjar, O.; Diab-Assaf, M.; Caldefie-Chezet, F.; Deloprt, L. *Int. J. Mol. Sci.* **2021**, *22* (22), 12200. DOI:10.3390/ijms222212200
(2) Costa, E. C.; Moreira, A. F.; Melo-Diogo, D de.; Gaspar, V. M.; Carvalho, M. P.; Correia, I. J. *Biotechnol. Adv.* **2016**, *34* (8), 1427–1441. DOI:10.1016/j.biotechadv.2016.11.002
(3) LaBarbera, D. V.; Reid, B. G.; Yoo,B. H. *Expert Opin. Drug Discov.* **2012**, *7*(9), 819–830. DOI:10.1517/17460441.2012.708334
(4) Szot, C. S.; Buchanan, C. F.; Freeman, J. W.; Rylander, M. N. *Biomaterials* **2011**, *32* (31),7905–7912. DOI:10.1016/j.biomaterials.2011.07.001
(5) Hutchinson, L.; Kirk, R. *Nat. Rev. Clin. Oncol.* **2011**, *8* (4), 189–190. DOI:10.1038/nrclinonc.2011.34
(6) Breslin, S.; O'Driscoll, L. *Drug Discov. Today.* **2013**, *18* (5–6), 240–249. DOI:10.1016/j.drudis.2012.10.003
(7) Kima, G. W.; Kimb, Y. J.; Kimb, H. K. *Appl. Sci. Converg. Technol.* **2021**, *30* (1), 1–5. DOI:10.5757/ASCT.2021.30.1.001
(8) Murphy, S. V.; Atala, A. *Nat. Biotechnol.* **2014**, *32* (8), 773–785. DOI:10.1038/nbt.2958
(9) Zhang, T.; Zhao, W.; Zhang, X. H.; Wang, X. W.; Zhang, K. X.; Yin, J. B. *Appl. Mater. Today* **2021**, *25*, 101227. DOI:10.1016/j.apmt.2021.101227
(10) Kang, D.; Hong, G.; An, S.; Jang, I.; Yun, W. S.; Shim, J. H.; Jin, H. *Small* **2020**, *16* (13), 1905505. DOI:10.1002/smll.201905505
(11) Singha, N. K.; Hanb, W.; Namc, S. A.; Kim, J. W.; Kim, J. Y.; Kim, Y. K.; Cho, D. W. *Biomaterials* **2020**, *232*, 119734. DOI:10.1016/j.biomaterials.2019.119734
(12) Ullah, F.; Javed, F.; Mushtaq, I.; et al. *Int. J. Biol. Macromol.* **2023**, *230*, 123131. DOI:10.1016/j.ijbiomac.2022.12313
(13) Ma, Y.; Wang, Y. L.; Chen, D. N.; et al. *J. Mater. Chem. B* **2023**, *11* (13), 2989–3000. DOI:10.1039/D2TB02200A
(14) Lee, J. Y.; Lee, H.; Jin, E.J.; Ryu, D.; Kim, G. H. *NPJ Regen. Med.* **2023**, *8* (1), 18. DOI:10.1038/s41536-023-00292-5
(15) Hwangbo, H.; Lee, H.; Jin, E. J.; Jo, Y.; Son, J.; Woo, H. M.; Ryu, D.; Kim, H. W. *Adv. Funct. Mater.* **2022**, *33* (10), 2209157. DOI:10.1002/adfm.202209157
(16) Gao, C.; Li, Y. X.; Liu, X. Y.; Huang, J.; Zhang, Z. J. *Chem. Eng. J.* **2023**, *451*, 138788. DOI:10.1016/j.cej.2022.138788
(17) Zhang, H. J.; Qin, C.; Zhang, M.; Han, Y. H.;Ma, J. G.; Wu, J. F.; Yao, Q. Q.; Wu, C. T. *Nano Today* **2022**, *46*, 101584. DOI:10.1016/j.nantod.2022.101584
(18) Chen, H. Y.; Gonnella, G.; Jie Huang, J.; Di-Silvio, L. *Biomimetics* **2023**, *8* (1), 87–100. DOI:10.3390/biomimetics8010087
(19) Hong, S.; Song, J. M. *Acta Biomater.* **2022**, *138* (15), 228–239. DOI:10.1016/j.actbio.2021.10.031
(20) Li, X.; et al. *Bio-des. Manuf.* **2020**, *3* (4), 361–372. DOI:10.1007/s42242-020-00085-5
(21) Liu, Q.; et al. *Bio-des. Manuf.* **2023**, *6* (4), 373–389. DOI:10.1007/s42242-022-00229-9
(22) Chae, S.; Cho, D. W. *MRS Bulletin* **2022**, *47* (1), 70–79. DOI:10.1557/s43577-021-00260-8
(23) Janani, G.; Priya, S.; Dey, S.; Mandal, B. B. *ACS Appl. Mater. Interfaces*. **2022**, *14*(8), 10167−10186. DOI:10.1021/acsami.2c00312
(24) Abelseth, E.; Abelseth, L.; De la Vega, L.; Beyer, S. T.; Wadsworth, S. J.; Willerth, S. M. *ACS Biomater. Sci. Eng.* **2019**, *5*(1), 234–243. DOI:10.1021/acsbiomaterials.8b01235
(25) He, J. Y.; Wang, J. L.; Pang, Y.; Yu, H.; Qin, X. Q.; Su, K.; Xu, T.; Ren, H. Z. *Int J Bioprint* .**2022**, *8*(3), 176-190. DOI:10.18063/ijb.v8i3.581
(26) Geevarghese, R.; Somasekharan, L. T.; Bhatt, A.; Kasoju, N.; Nair, R. P. *Int. J. Biol. Macromo.* **2022**, *207*, 278–288. DOI:10.1016/j.ijbiomac.2022.02.191
(27) Fan, Z. C.; Wei, X. Y.; Chen, K. K.; Wang, L.; Xu, M. E. *Micromachines.* **2023**, *14*(4), 878-890. DOI:10.3390/mi14040878
(28) Liu, X.; Michael, S.; Bharti, K.; Ferrer, M.; Song, M. J. *Biofabrication*. **2020**, *12*(3), 035002. DOI:10.1088/1758-5090/ab76a1
(29) Deng, Q.; Luo, Y.; Zhang, X. Polym. Eng. Sci. **2020**, 61 (1), 167-172. HYPERLINK "https://doi.org/10.1002/pen.25565" DOI: 10.1002/pen.25565

Bioinks

TissueFab® Bioink - Conductive

Description	Composition	Contains	Cat. No.
UV/365 nm	GelMA, CNTs	≤5 CFU/g Bioburden (Fungal) ≤5 CFU/g Bioburden (Total Aerobic)	**915963**
UV/365 nm	GelMA, CNTs	≤5 CFU/g Bioburden (Fungal) ≤5 CFU/g Bioburden (Total Aerobic) <50 EU/mL Endotoxin	**926051**
Vis/405 nm	GelMA, CNTs	≤5 CFU/g Bioburden (Fungal) ≤5 CFU/g Bioburden (Total Aerobic)	**915726**
Vis/405 nm	GelMA, CNTs	≤5 CFU/g Bioburden (Fungal) ≤5 CFU/g Bioburden (Total Aerobic) <50 EU/mL Endotoxin	**926078**

TissueFab® Bioink - Bone

Description	Composition	Contains	Cat. No.
Vis/405 nm	PCL, Hydroxyapetite		**915033**
UV/365 nm	GelMA, Hydroxyapetite	≤5 CFU/g Bioburden (Fungal) ≤5 CFU/g Bioburden (Total Aerobic)	**915637**
UV/365 nm	GelMA, Hydroxyapetite	≤5 CFU/g Bioburden (Fungal) ≤5 CFU/g Bioburden (Total Aerobic) <50 EU/mL Endotoxin	**915025**
Vis/405 nm	GelMA, Hydroxyapetite	≤5 CFU/g Bioburden (Fungal) ≤5 CFU/g Bioburden (Total Aerobic)	**926086**
Vis/405 nm, low endotoxin	GelMA, Hydroxyapetite	≤5 CFU/g Bioburden (Fungal) ≤5 CFU/g Bioburden (Total Aerobic) <50 EU/mL Endotoxin	**926035**

TissueFab® Bioink - Facile Curable

Description	Composition	Contains	Cat. No.
Cationic Crosslinking	Gelatin	≤5 CFU/g Bioburden (Fungal) ≤5 CFU/g Bioburden (Total Aerobic)	**928437**
Facile Curable GelHA, Ionic	gelatin, hyaluronic acid	≤5 CFU/g Bioburden (Fungal) ≤5 CFU/g Bioburden (Total Aerobic) <50 EU/mL Endotoxin	**930016**

TissueFab® Bioink - General

Description	Composition	Contains	Cat. No.
Fibronectin - UV/365nm	GelMA, Fibroconectin	≤5 CFU/g Bioburden (Fungal) ≤5 CFU/g Bioburden (Total Aerobic) <50 EU/mL Endotoxin	**927066**
Alg(Gel)ma - UV/365 nm	GelMA, Alginate	≤5 CFU/g Bioburden (Fungal) ≤5 CFU/g Bioburden (Total Aerobic)	**926159**
(Gel)ma - UV/365 nm	GelMA	≤5 CFU/g Bioburden (Fungal) ≤5 CFU/g Bioburden (Total Aerobic)	**905429**
(GelAlg)ma - UV/365 nm	GelMA, AlgMA	<5 CFU/g Bioburden	**920983**
(GelAlg)ma - Vis/405 nm	GelMA, AlgMA	≤5 CFU/g Bioburden (Fungal) ≤5 CFU/g Bioburden (Total Aerobic)	**921610**
(GelAlgHA)ma - UV/365 nm	GelMA, AlgMA, HAMA	≤5 CFU/g Bioburden (Fungal) ≤5 CFU/g Bioburden (Total Aerobic)	**920975**
(GelAlgHA)ma - Vis/405 nm	GelMA, AlgMA, HAMA	<5 CFU/g Bioburden	**922862**
(GelHA)ma - UV/365 nm	GelMA, HAMA	≤5 CFU/g Bioburden (Fungal) ≤5 CFU/g Bioburden (Total Aerobic)	**919632**
(GelHA)ma - Vis/405 nm	GelMA, HAMA	≤5 CFU/g Bioburden (Fungal) ≤5 CFU/g Bioburden (Total Aerobic)	**919624**
Alg(Gel)ma - UV/365 nm	GelMA, Alginate	≤5 CFU/g Bioburden (Fungal) ≤5 CFU/g Bioburden (Total Aerobic)	**905410**
Alg(Gel)ma - Vis/525 nm	GelMA, Alginate	≤5 CFU/g Bioburden (Fungal) ≤5 CFU/g Bioburden (Total Aerobic)	**906913**
Sacrificial	Pluronic	≤5 CFU/g Bioburden (Fungal) ≤5 CFU/g Bioburden (Total Aerobic)	**906905**

TissueFab® Bioink - General, Low Endotoxin

Description	Composition	Contains	Cat. No.
Crosslinking solution, low endotoxin	Alginate	≤5 CFU/g Bioburden (Fungal) ≤5 CFU/g Bioburden (Total Aerobic) <25 EU/mL Endotoxin	**919926**
GelMA-UV bioink, low endotoxin	GelMA	≤5 CFU/g Bioburden (Fungal) ≤5 CFU/g Bioburden (Aerobic) ≤50 EU/mL Endotoxin	**925217**
GelMA-UV bioink, low endotoxin	GelMA	≤5 CFU/g Bioburden (Fungal) ≤5 CFU/g Bioburden (Total Aerobic) <50 EU/mL Endotoxin	**927066**
(GelAlg)ma - Vis/405nm, low endotoxin	GelMA, Alginate	≤5 CFU/g Bioburden (Fungal) ≤5 CFU/g Bioburden (Total Aerobic) <50 EU/mL Endotoxin	**927228**
GelAlg - LAP, low endotoxin	GelMA, Alginate	<5 cfu/mL Bioburden <50 EU/mL Endotoxin	**925055**
(GelAlgHA)MA Vis/405 nm, low endotoxin	GelMA, Alginate, Hyaluronic acid	≤5 CFU/g Bioburden (Fungal) ≤5 CFU/g Bioburden (Total Aerobic) <50 EU/mL Endotoxin	**927252**
(GelHA)ma -Vis/405nm, low endotoxin	GelMA, Hyaluronic acid		**927201**
(Gel)ma - VIS/405nm, low endotoxin	GelMA, LAP	≤5 CFU/g Bioburden (Fungal) ≤5 CFU/g Bioburden (Total Aerobic) <50 EU/mL Endotoxin	**918741**

TissueFab® Bioink Kit

Description	Contains	Contains	Cat. No.
(Gel)ma Fibrin - Vis/405, low endotoxin	GelMA, Fibrinogen	≤10 CFU/g Bioburden (Fungal) ≤10 CFU/g Bioburden (Total Aerobic) <125 EU/mL Endotoxin	**927074**
(Gel)ma Fibronection - Vis/405 nm, low endotoxin	GelMA, Fibronectin	≤5 CFU/g Bioburden <50 EU/mL Endotoxin	**926019**
(Gel)ma Laminin - UV/365 nm, low endotoxin	GelMA, Laminin	≤5 CFU/g Bioburden (Fungal) ≤5 CFU/g Bioburden (Total Aerobic)	**927058**
(Gel)ma Laminin - Vis/405 nm, low endotoxin	GelMA, Laminin	<50 EU/mL Endotoxin ≤5 CFU/g Bioburden <50 EU/mL Endotoxin	**926000**

Functionalized Natural Polymers

Gelatin Methacrylate (GelMa)

Name	Gel Strength (g Bloom)	Degree of Substitution	Cat. No.
Gelatin methacryloyl	90-110	60%	**900628**
	170–195	60%	**900741**
	300	40%	**900629**
	300	60%	**900622**
	300	80%	**900496**

Gelatin Methacrylate (GelMa) - low endotoxin

Name	Description	Form	Contains	Cat. No.
Low endotoxin GelMA, Type A	Degree of substitution 80%	Powder or chunks	Bioburden <10 CFU/g Endotoxin <125 EU/g	**918636**
Low endotoxin GelMA, Type B	Degree of substitution 80%	Powder, chunks, or fibers	Bioburden <10 CFU/g Endotoxin <125 EU/g	**920045**
Low endotoxin GelMA solution, Type B	Degree of substitution 80%	Viscous liquid	Bioburden <5 CFU/g Endotoxin <25 EU/g	**922188**
Low endotoxin GelMA, mol wt 95 kDa	Degree of substitution 60%	Powder	Endotoxin <10 EU/g	**918628**

Alginate Methacrylate

Description	Degree of Methacrylation	Cat. No.
Low viscosity	10-30%	**911968**
Medium viscosity	10-30%	**913057**
High viscosity	20-40%	**912387**

Alginate Methacrylate - low endotoxin

Description	Degree of Methacrylation	Contains	Cat. No.
Medium Viscosity	15-25%	<10 CFU/g Bioburden (Aerobic) <10 CFU/g Bioburden (Fungal) <100 EU/g Endotoxin	**924482**

Hyaluronic acid Methacrylate

Molecular Weight (M_w)	Degree of Methacrylation	Cat. No.
40,000-70,000	20-50%	**914568**
140,000-190,000	20-50%	**914304**
170,000-250,000	10-30%	**914800**

Hyaluronic acid Methacrylate - low endotoxin

Description	Particle Size	Contains	Cat. No.
Low Viscosity	0.2 µm	<10 CFU/g Bioburden (Aerobic) <10 CFU/g Bioburden (Fungal) <100 EU/g Endotoxin	**924490**

Functionalized PEGs

Multiarm PEGs

Functional Group	Shape	Average M_n	Cat. No.
acrylate	4-arm	10,000	**JKA7068**
	4-arm	20,000	**JKA7034**
	8-arm	20,000	**JKA10016**
acrylate (hexaglycerol core)	8-arm	5,000	**JKA8062**
acrylate (tripentaerythritol core)	8-arm	5,000	**JKA10055**
acrylate (tripentaerythritol core)	8-arm	10,000	**JKA10021**
maleimide	4-arm	20,000	**JKA7029**
	4-arm	40,000	**JKA7067**
	8-arm	40,000	**JKA8029**
maleimide (hexaglycerol core)	8-arm	10,000	**JKA8027**
maleimide (tripentaerythritol core)	8-arm	10,000	**JKA10018**
methacrylate (hexaglycerol core)	8-arm	5,000	**JKA8063**
	8-arm	10,000	**JKA8064**
methacrylate (tripentaerythritol core)	8-arm	5,000	**JKA10056**
	8-arm	10,000	**JKA10057**
NH2 (hexaglycerol core)	8-arm	10,000	**JKA8008**
NH2 (tripentaerythritol core)	8-arm	10,000	**JKA10001**
norbornene	4-arm	10,000	**808474**
SH	4-arm	5,000	**JKA7002**
	4-arm	10,000	**565725**
	8-arm	20,000	**JKA8007**
SH (pentaerythritol core)	4-arm	10,000	**JKA7008**
SH (tripentaerythritol core)	8-arm	10,000	**JKA10022**

PEG Acrylates

Name	Average M_n	Cat. No.
Acrylate-PEG3500-Acrylate	3,500	**JKA4048**
Poly(ethylene glycol) diacrylate	1,000	**729086**
	2,000	**701971**
	20,000	**767549**
	6,000	**701963**
Poly(ethylene glycol) dimethacrylate	20,000	**725692**

Clickable PEGs

Name	Average M_n	Cat. No.
HS-PEG1500-SH	1,500	**JKA4105**
Poly(ethylene glycol) dithiol	1,000	**717142**
	3,400	**704539**

Photoinitiators

Functional Group	Description	Cat. No.
Lithium phenyl-2,4,6-trimethylbenzoylphosphinate	>=95%	**900889**
Water-soluble TPO based nanoparticle photoinitiator	contains ionic surfactant	**906808**
	contains nonionic surfactant	**906816**

PRINTING A BRIGHTER FUTURE

3D Bioprinting Handbook

In this guide, we explore the potential for 3D bioprinting to advance biomaterials research. Reviews by leading researchers and protocols designed by leading R&D experts in Bioprinting. This handbook is intended for all levels of researchers, both experts and nonexperts in tissue engineering and *in-vitro* models for drug discovery.

FEATURED ARTICLES

- Design of Blinks for Bloprinting
- 3D Bioprinting of Functional Tissue Models
- Hybrid printing for Engineering Vascularized Tissue Constructs
- Recent Advances in 3D Biofabrication of Blood vessels

Order your complimentary copy from:
SigmaAldrich.com/3dbp-handbook

MK_BR12642EN

The Life Science business of Merck operates as MilliporeSigma in the U.S. and Canada.

Sigma-Aldrich®
Lab & Production Materials